Emergent electronic and magnetic response in antiferromagnet-proximitized SrIrO3 and Cu-based quasi 2D hybrid perovskites

Debakanta Samal

Institute of Physics (IoP), Bhubaneswar, India.

Outline

- **Antiferromagnetic proximity effect involving spin-orbit semimetal $SrIrO_3$**
- **Enhanced phase coherence length in $SrCuO_2/SrIrO_3$**
- **Emergent topological response in $SrCuO_2/SrIrO_3$**
- **Organic-inorganic hybrid perovskites: quasi-2D magnets**
- **Contrasting magnetism in Cu-based systems ($A_2CuX_{4;}$ X = Cl, Br)**
- **Possible non-collinear magnetic structure**

Acknowledgement

Subhadip Jana (IoP,Bhubaneswar)
Sachin Sarangi
Tapas Senapati (NISER, Bhubaneswar)
Kartik Senapati
Shwetha Bhat (IISc, Bangalore)

Antiferromagnet proximitized $SrIrO_3$
Phys. Rev. B 107, 134415 (2023)

Pujalin Biswal (IoP, Bhubaneswar)
Sachin Sarangi
Goutam Tripathy
Diptikant Swain (ICT, Bhubaneswar)
Ashis Kumar Nandy (NISER, Bhubaneswar)
Sagar Sarkar (Uppsala University)
S D Mahanti (Michigan State University)

Cu-based quasi 2D hybrid perovskites (unpublished)

Generous funding

Spin-orbit coupling: a relativistic effect

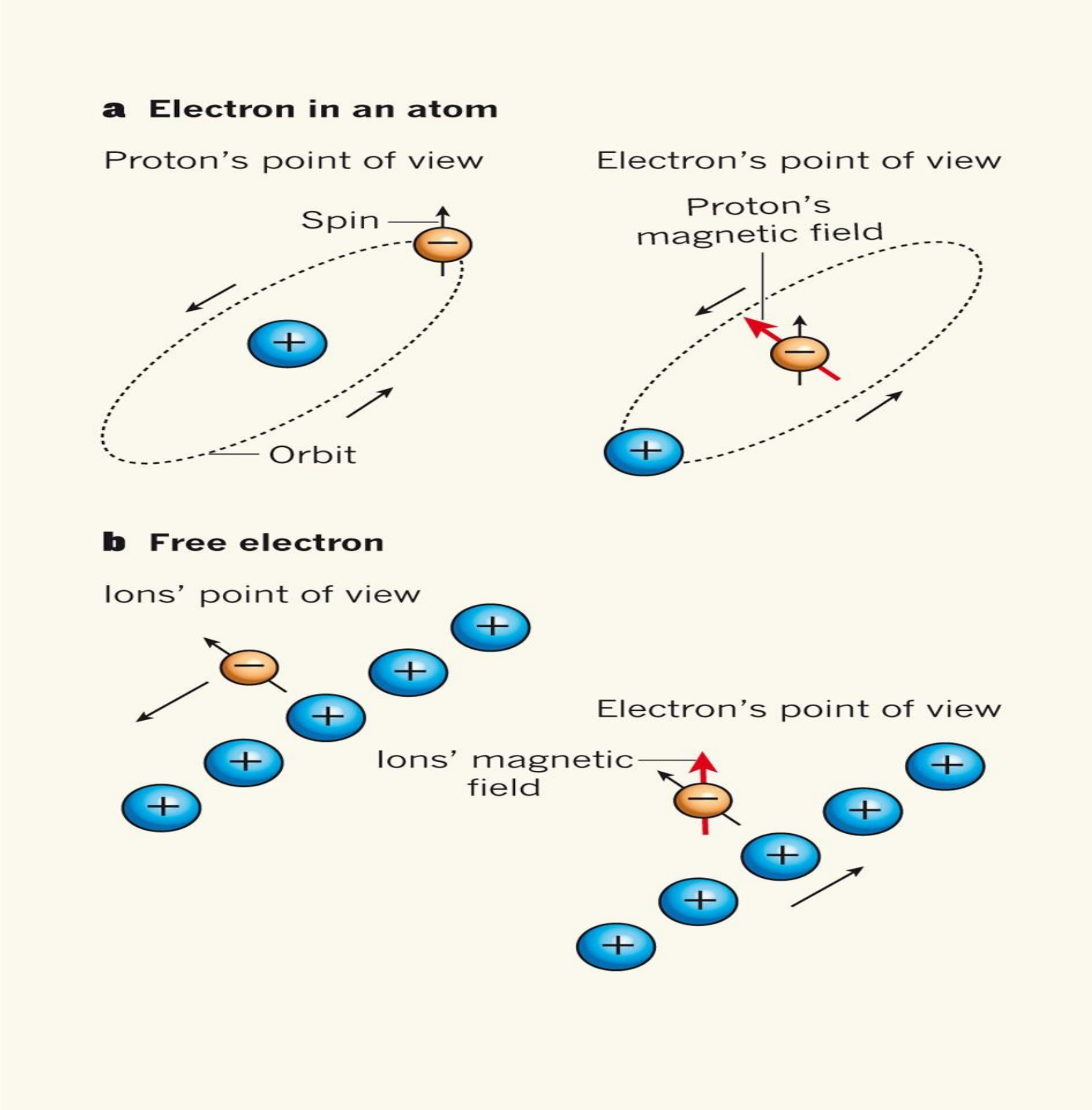

M Chapman and Carlo Sa de Melo Nature 471, 41–42 (2011)

$$\mathbf{B}' = -\frac{-\mathbf{v}}{c^2} \times \mathbf{E},$$

$$\begin{aligned} H_{SO} &= -\boldsymbol{\mu}_S \cdot \mathbf{B}' \\ &= -\left(-\frac{e\hbar}{2m}\boldsymbol{\sigma}\right) \cdot \left(-\frac{1}{c^2}(-\mathbf{v}) \times \mathbf{E}\right) \\ &= -\frac{e\hbar}{2m^2c^2}\boldsymbol{\sigma} \cdot (\mathbf{E} \times \mathbf{p}) \end{aligned}$$

$$\langle\psi|V_{SOI}|\psi\rangle_{nls} \sim Z^4$$

Range of energies for various interactions present in solid

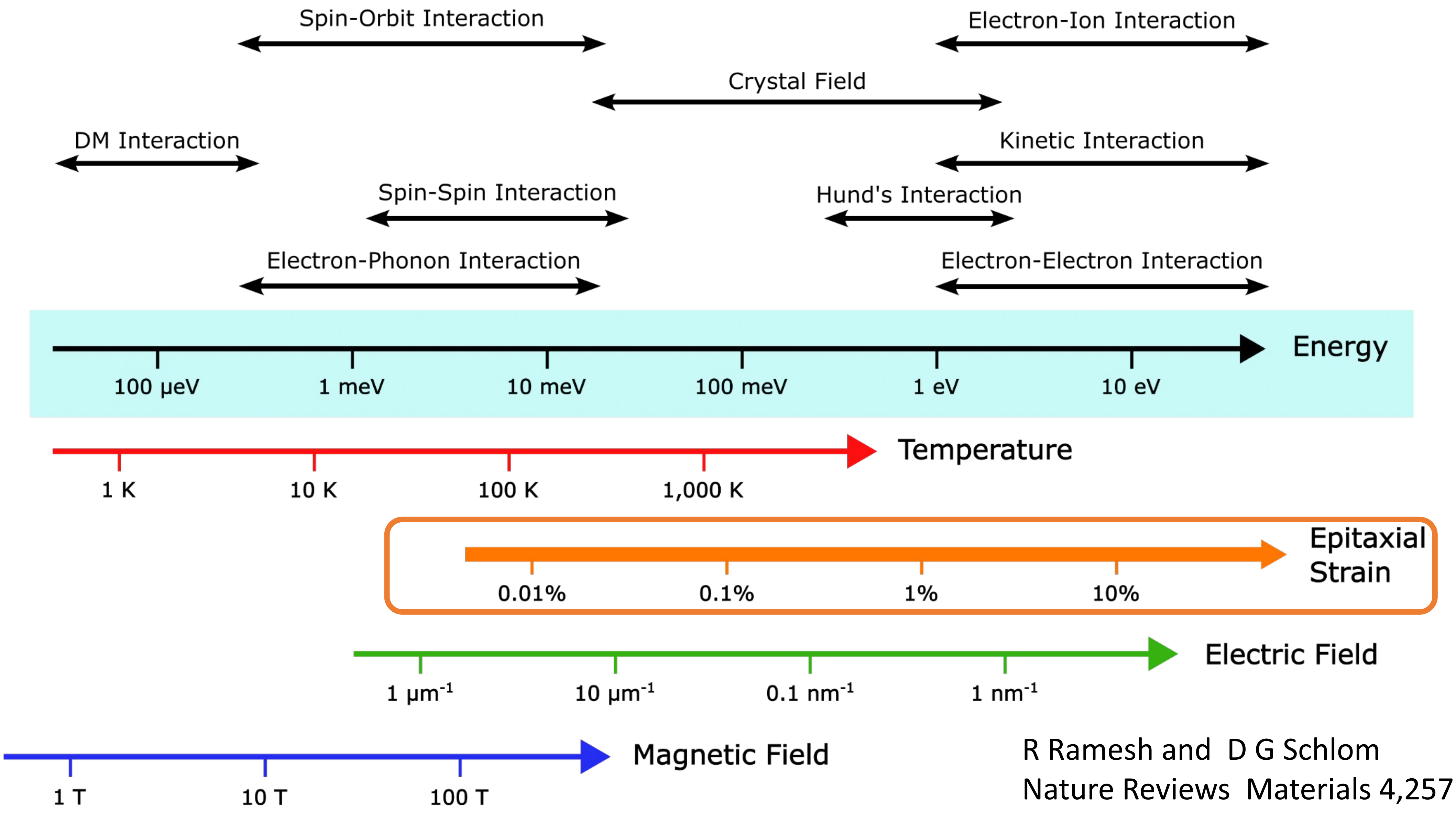

R Ramesh and D G Schlom
Nature Reviews Materials 4,257 (2019)

Hierarchy in spin-orbit coupling strength

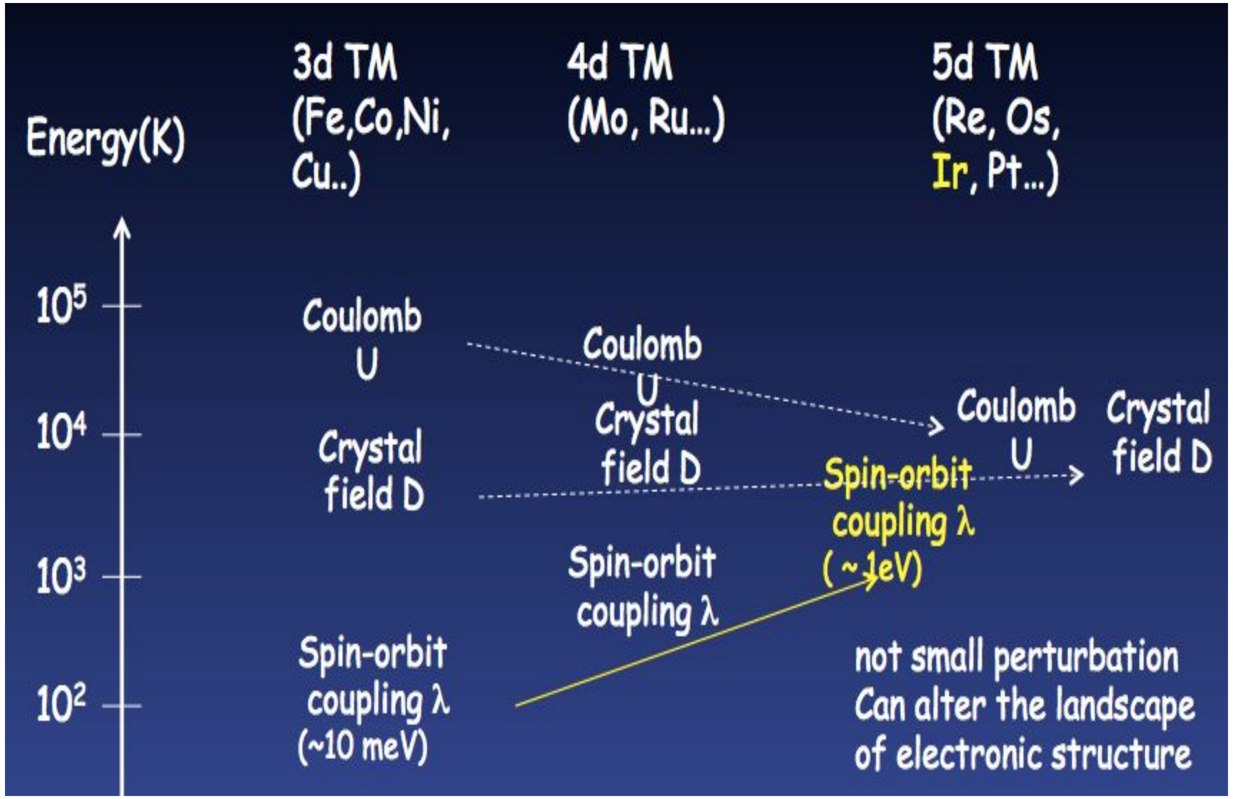

Figure Courtesy : Prof. Takagi

Interaction	3d(e.g. Cu)	5d (e.g. Ir)
Coulomb intercation (U)	3-5 eV	1-2 eV
Spin-orbit coupling (λ)	0.01 eV	0.5 eV
Crystal field splitting	1-2 eV	1-4 eV

Spin-orbit Mott insulator Sr_2IrO_4

Sr_2CoO_4	Sr_2RhO_4	Sr_2IrO_4
Metal	Metal	Insulator

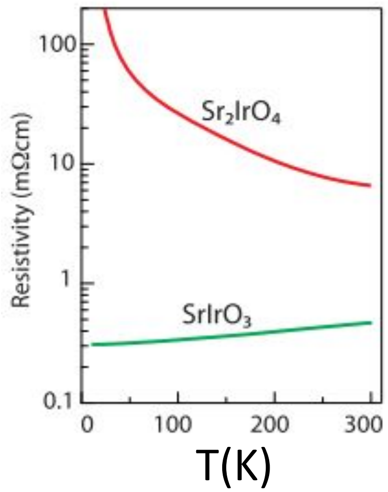

Nie *et al.* PRL 114, 016401 (2015)

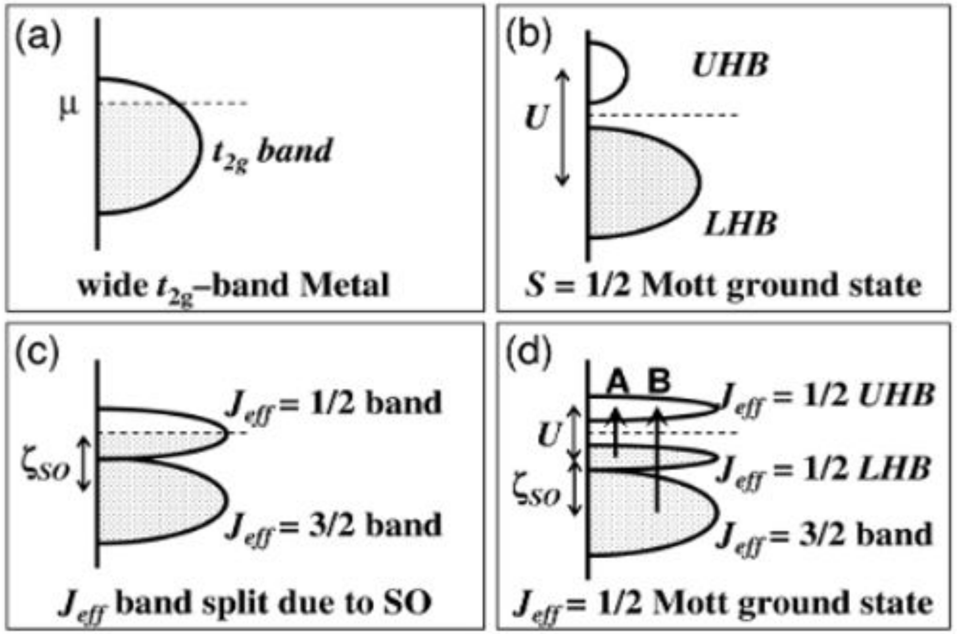

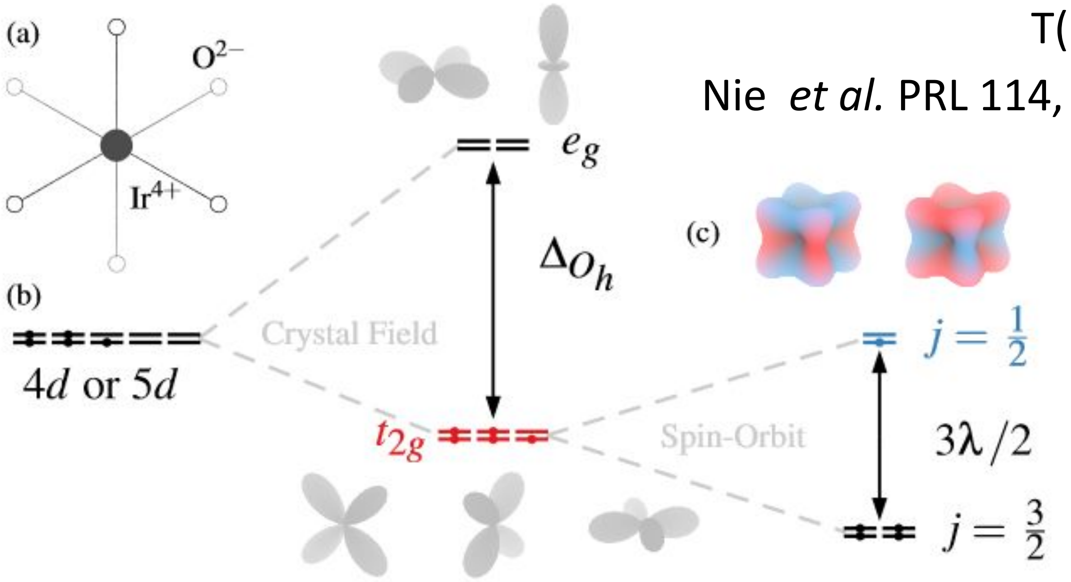

Sr_2IrO_4 spin-orbit Mott insulator

Kim *et al.* PRL 101,076402, 2008

Rau *et al.* Annual Review of Condensed Matter Physics, 2016

Novel phases induced by strong spin-orbit coupling in iridates

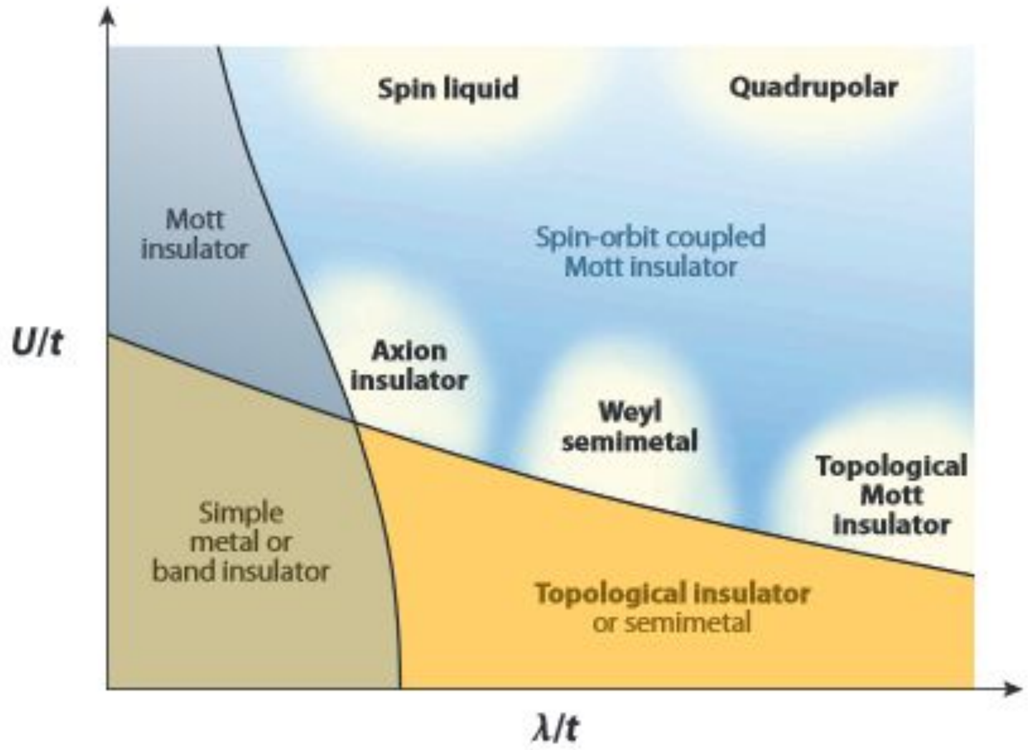

W. Witczak-Krempa et al., An. Rev. Cond. Mat. 5,57 (2014)

Thin Films (111) of Pyrochlore Iridates

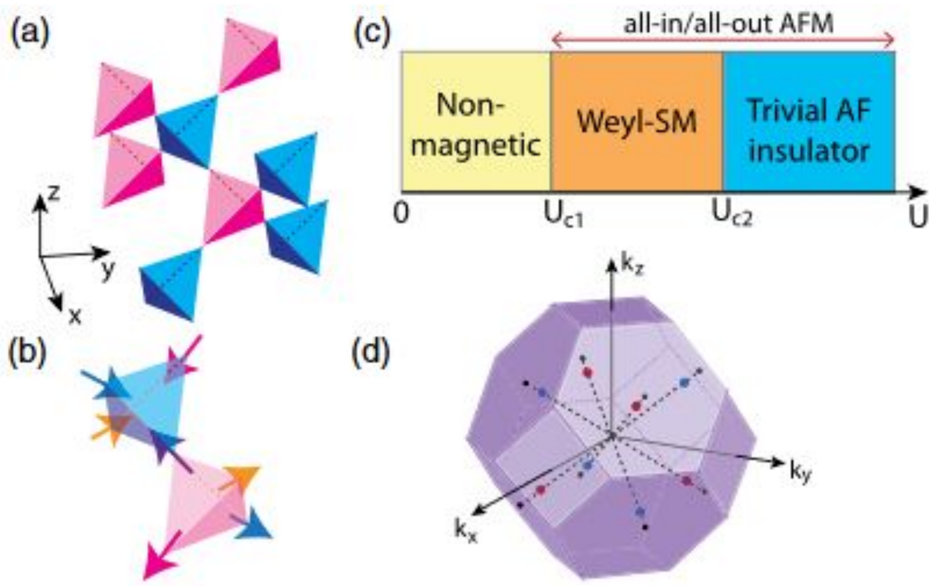

B. Yang *et al.*, PRL 112, 246402 (2014)

$SrIrO_3$ ($Sr_{n+1}Ir_nO_{3n+1}$, n=∞)

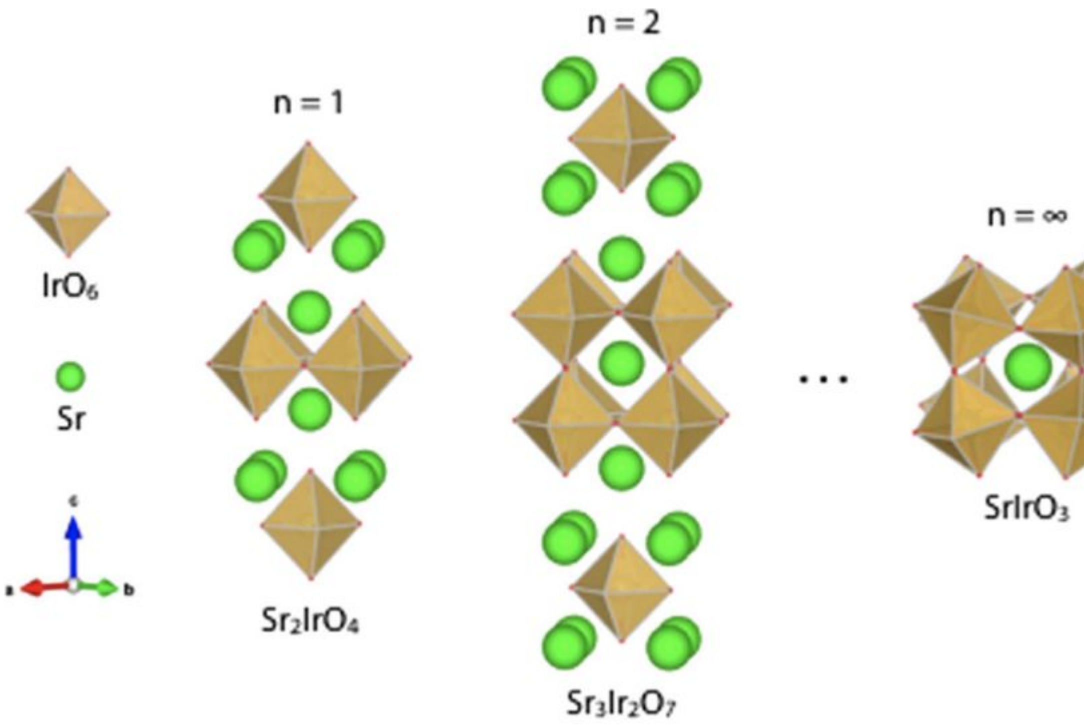

Ruddlesden-Popper (RP) phases

Liu *et al.*, PRM 1, 075004 (2017)

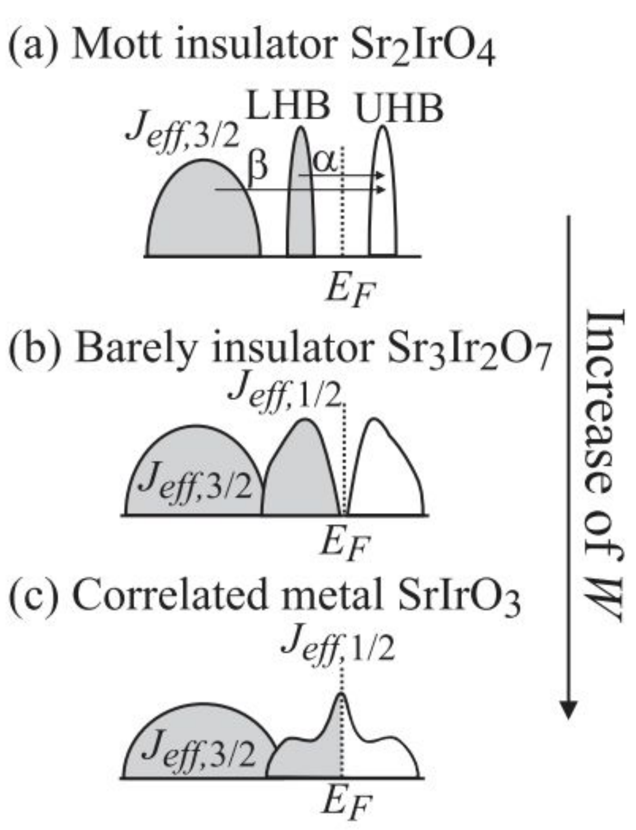

S. J. Moon *et al.*, PRL 101, 226402 (2008)

$SrIrO_3$ ($Sr_{n+1}Ir_nO_{3n+1}$; n=∞): spin-orbit semimetal

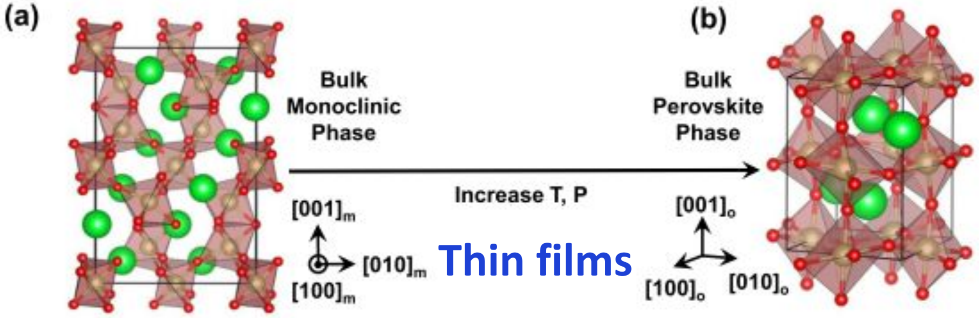

Appl. Phys. Lett. 108, 151604 (2016)

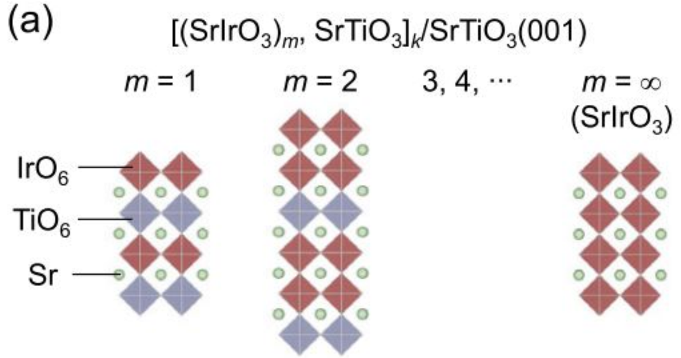

Engineering a Spin-Orbital Magnetic Insulator by Tailoring Superlattices

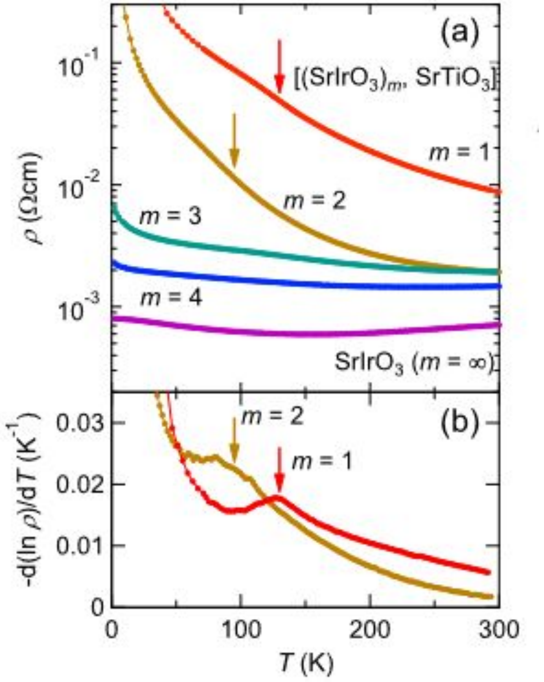

J. Matsuno *et al.*, PRL 114, 247209 (2015)

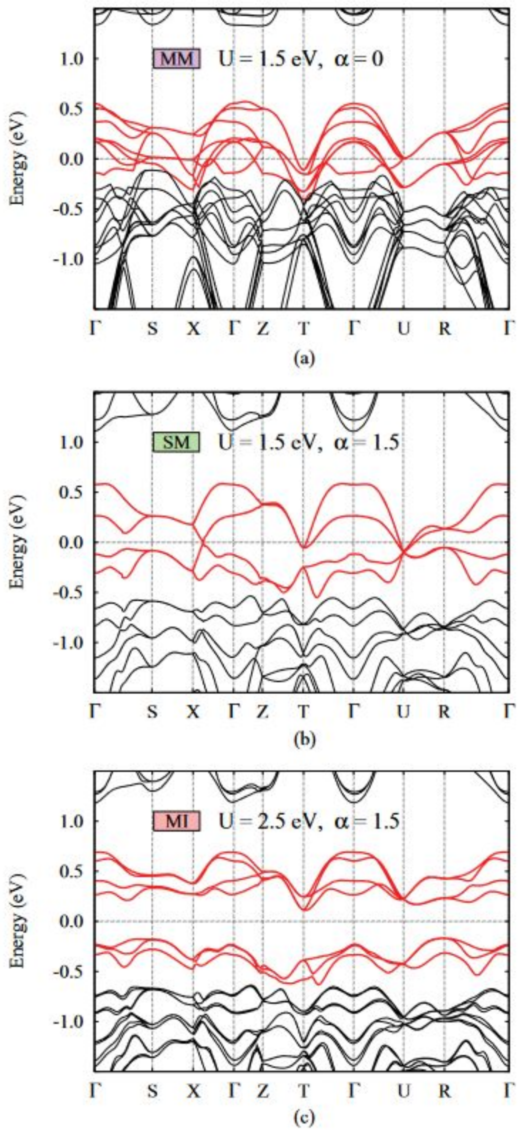

M. A. Zeb *et al.*, PRB 86,085149 (2012)

Perovskite $SrIrO_3$: correlated spin-orbit semimetal

- Narrow band semimetal with steep linear dispersion (PRL 114,016401 (2015))
- Signature for Dirac fermion like quasi particles from magneto-transport measurements is not evident.
- “Antiferromagnetic proximity effect” induces emergent topological electron transport

Quenching of magnetic impurity scattering

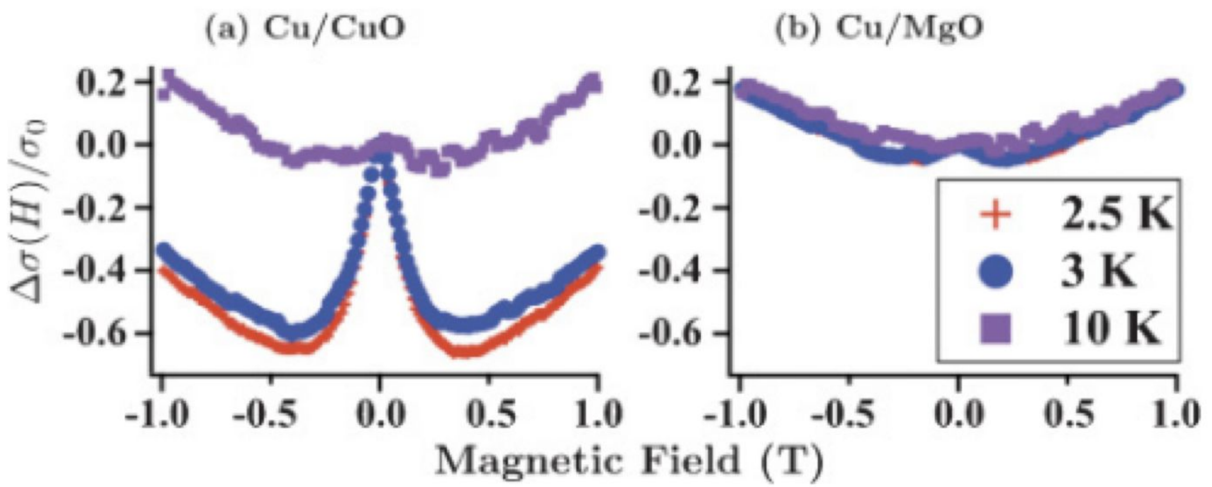

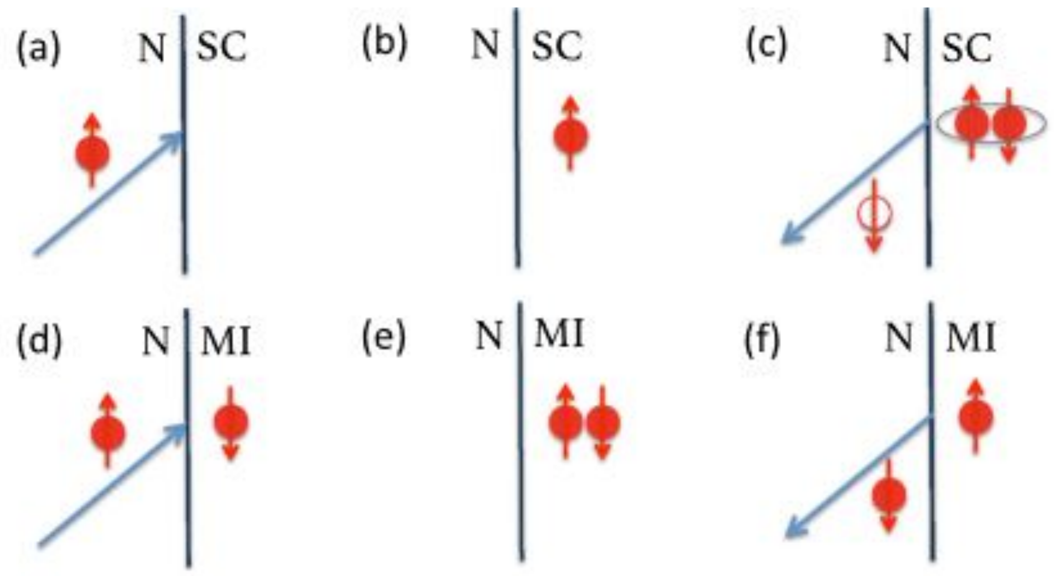

Spin Andreev-like Reflection in Metal-Mott Insulator Heterostructure

K. A. Al-Hassanieh *et al.* PRL 114, 066401 (2015)

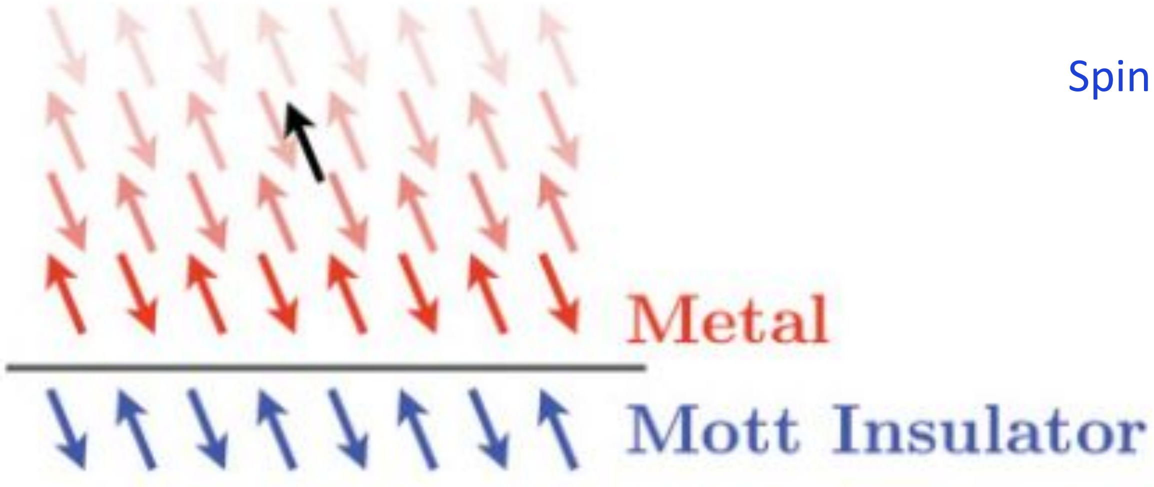

	$\tau_s\ (10^{-12}\,s)$
Cu/CuO:	$(7.1 \pm 0.4) \times 10^1$
Cu/MgO:	4.6 ± 0.8

K.Munakata *et al.*PRB 84, 161405(R) (2011)

$SrCuO_2$(antiferromagnet)/$SrIrO_3$ bilayer

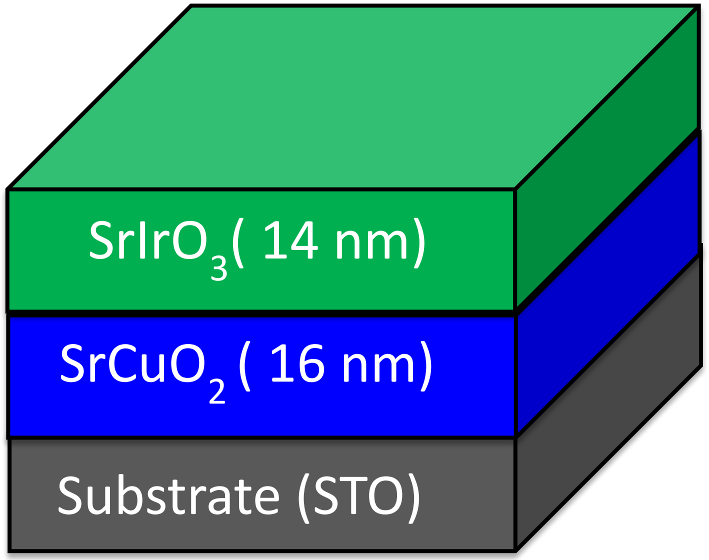

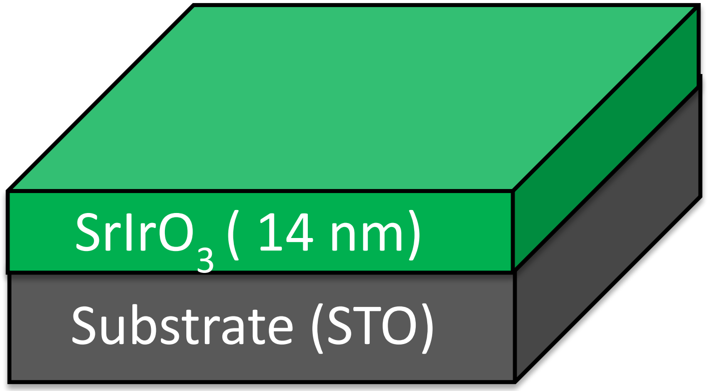

a_{pc} (SIO)= 3.96 Å
a (SCO)=3:926 Å

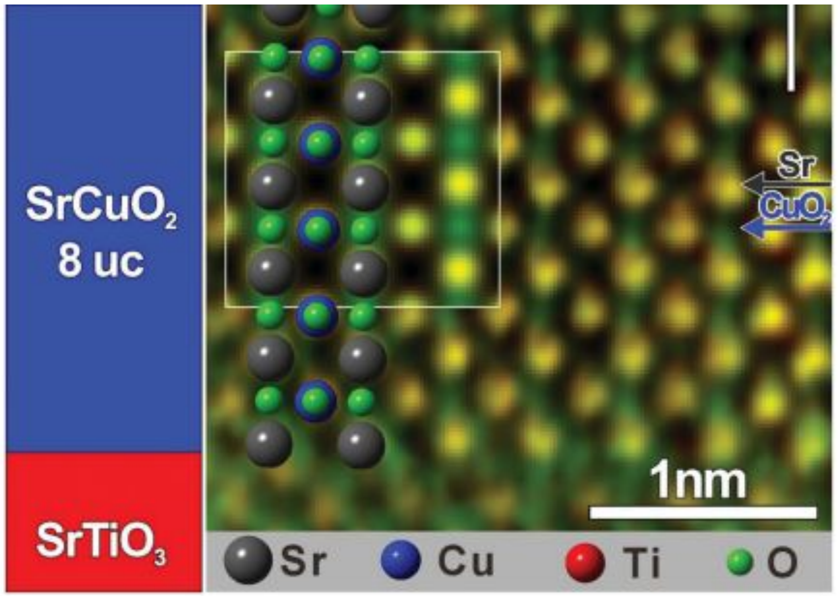

D. Samal et al.,
PRL 111, 096102 (2013)

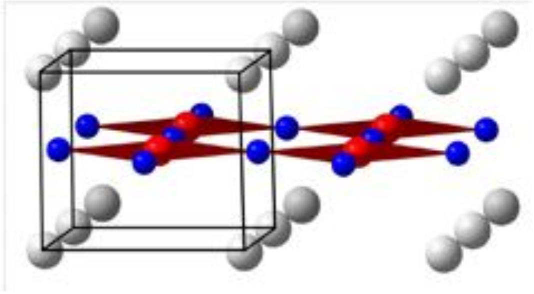

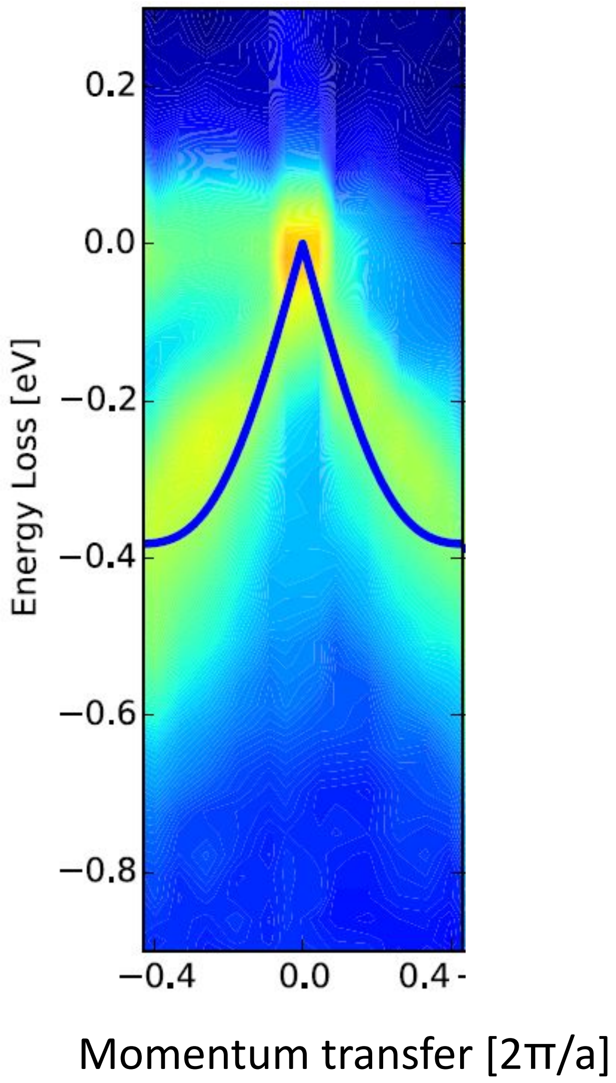

M. Dantz et al., Scientific reports 6, 32896 (2016)

Growth and structural characterization of $SrCuO_2/SrIrO_3$ bilayer

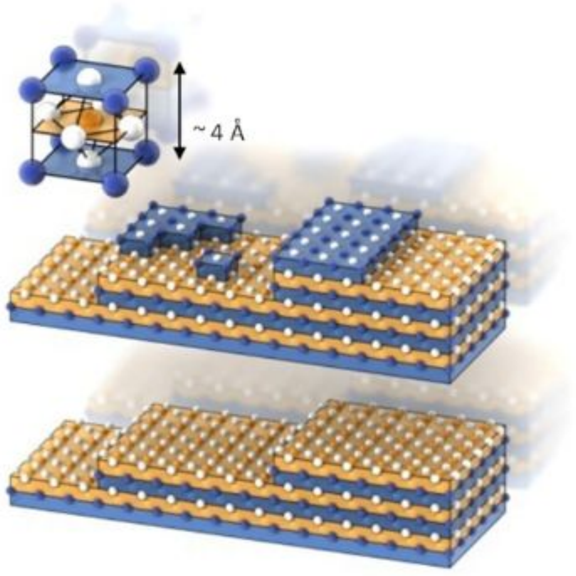

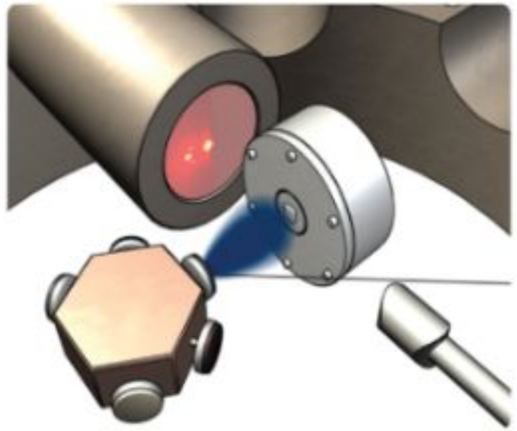

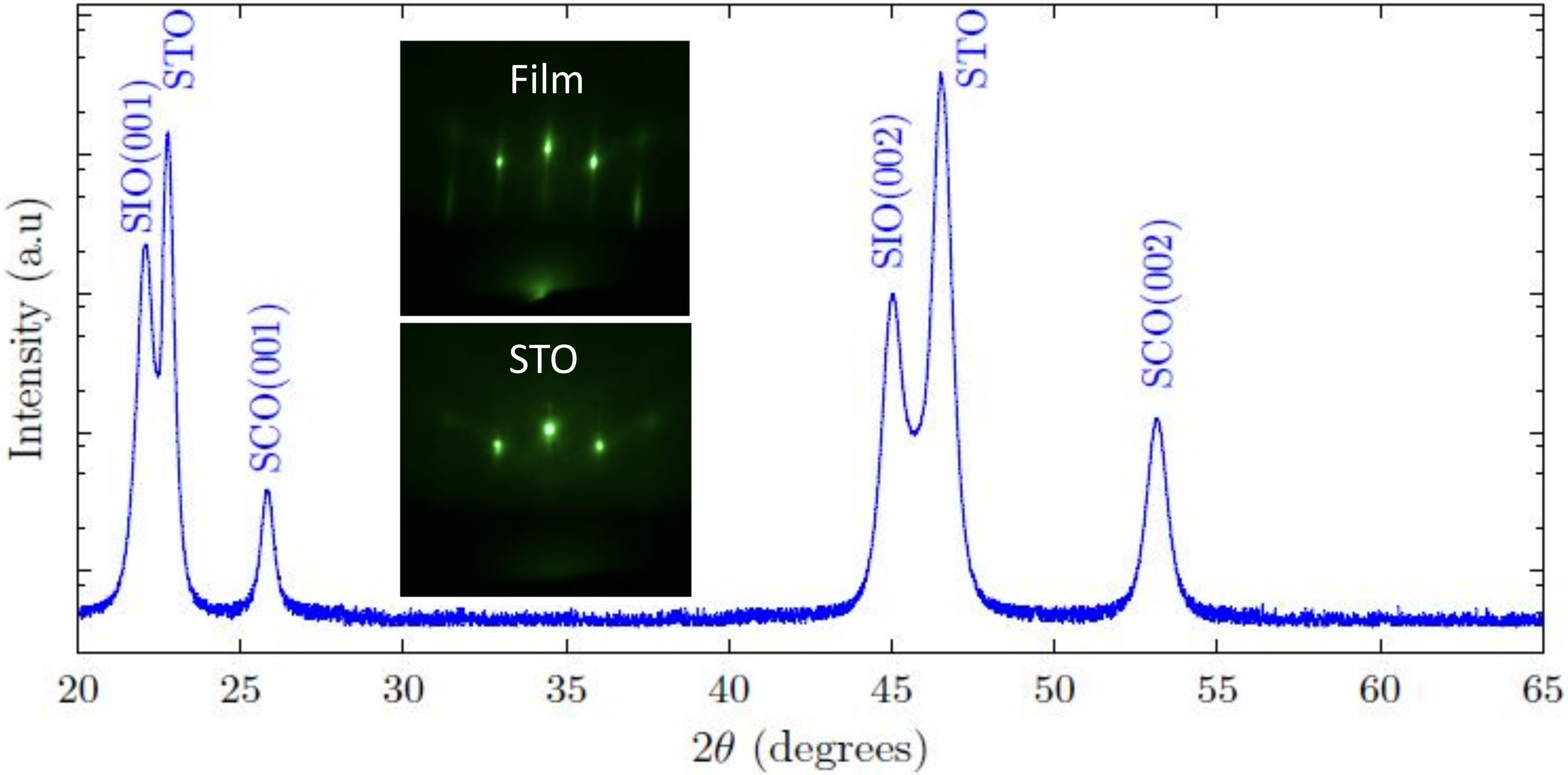

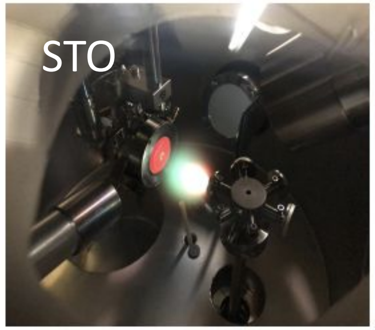

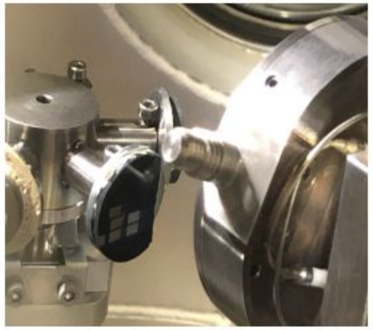

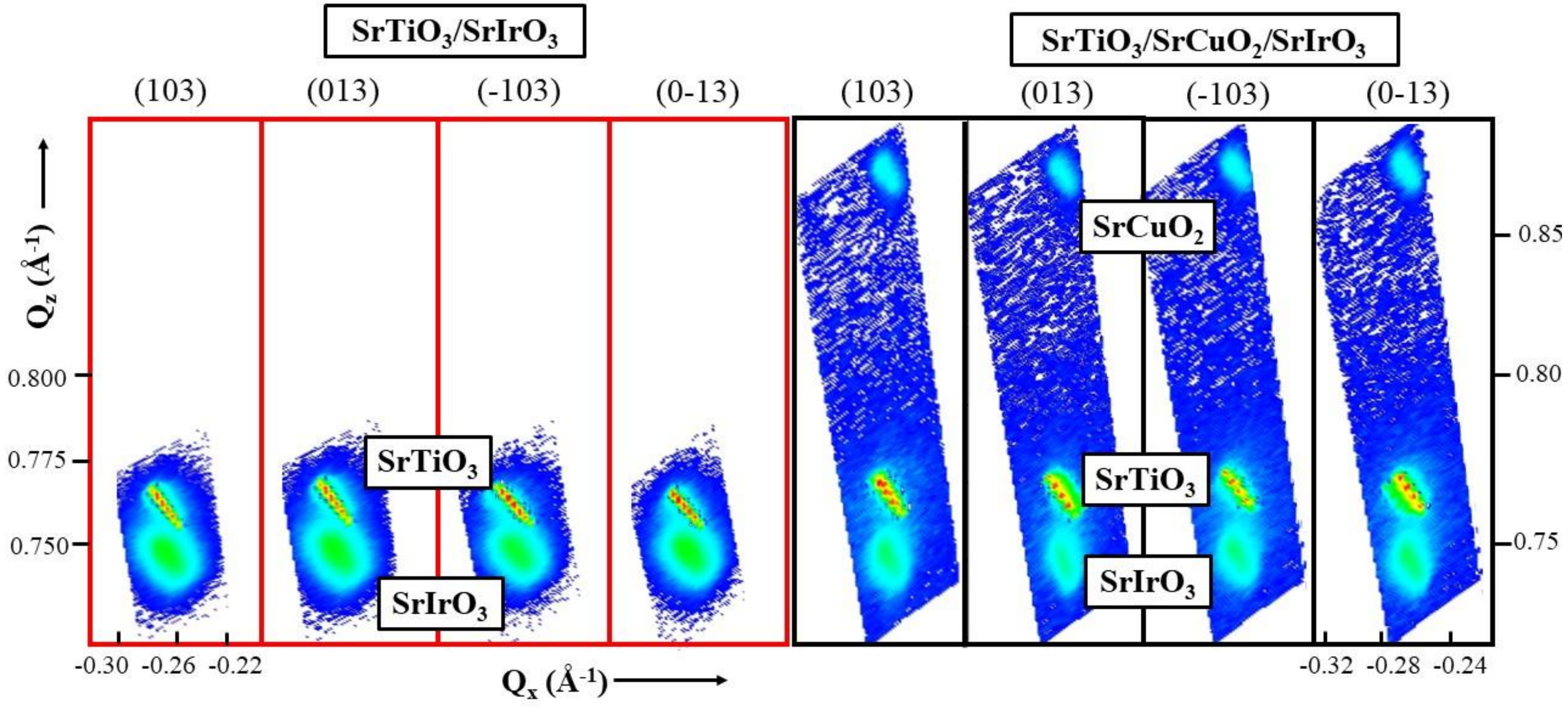
SrTiO3/SrIrO3
SrTiO3/SrCuO2/SrIrO3
(103)
(013)
(-103)
(0-13)
(103)
(013)
(-103)
(0-13)
Qz (Å-1)
0.800
0.775
0.750
SrTiO3
SrIrO3
SrCuO2
SrTiO3
SrIrO3
0.85
0.80
0.75
-0.30 -0.26 -0.22
Qx (Å-1)
-0.32 -0.28 -0.24

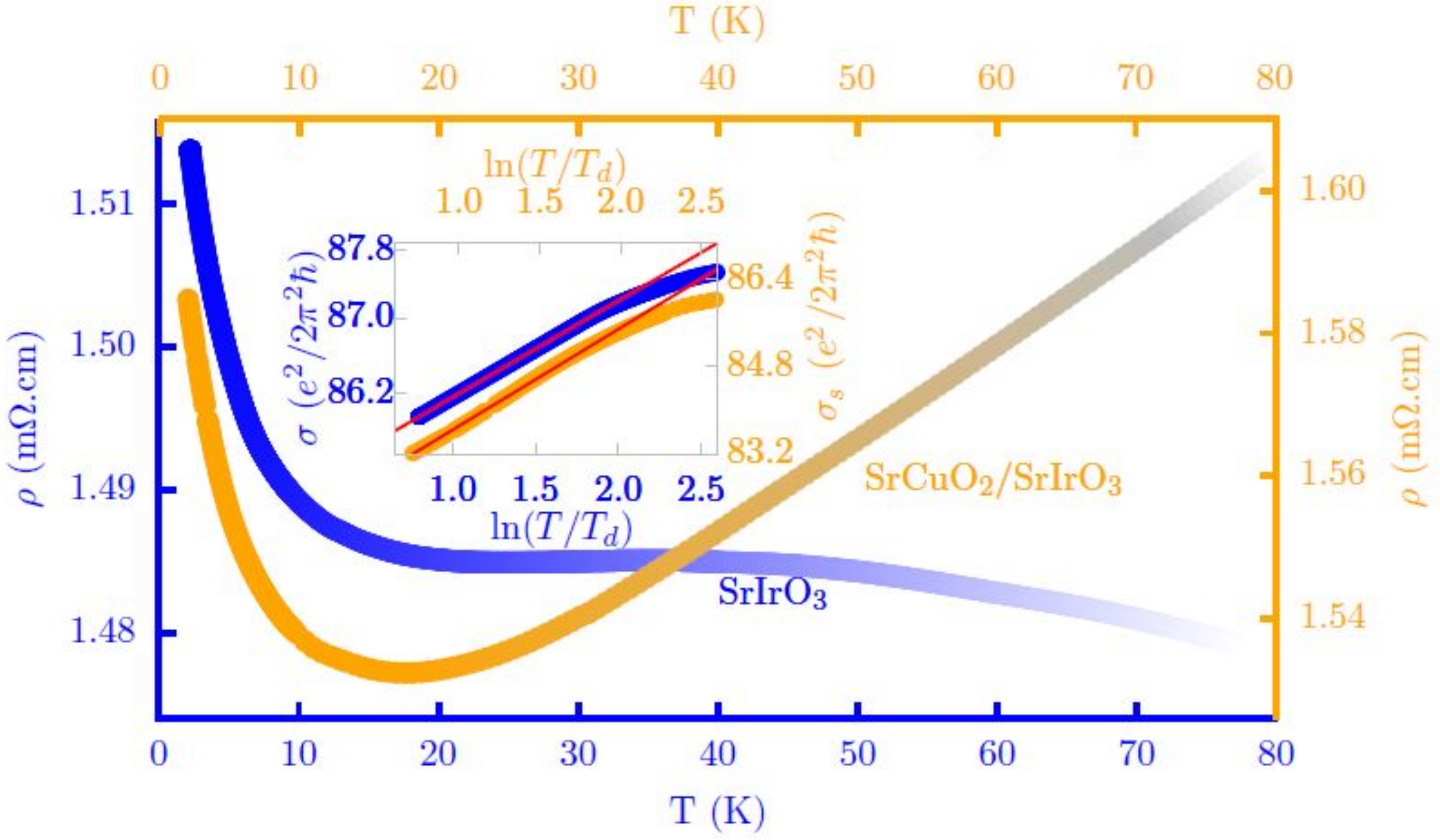

$n \sim 3.7 \times 10^{19}\ cm^{-3}$

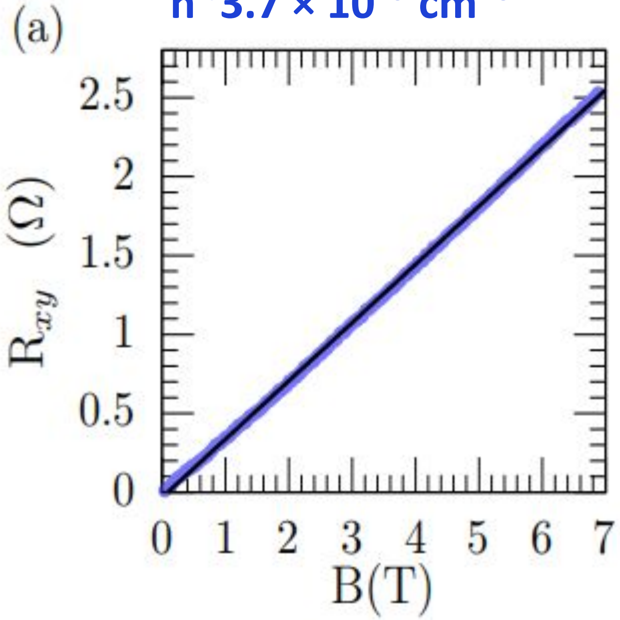

$n \sim 4 \times 10^{19}\ cm^{-3}$

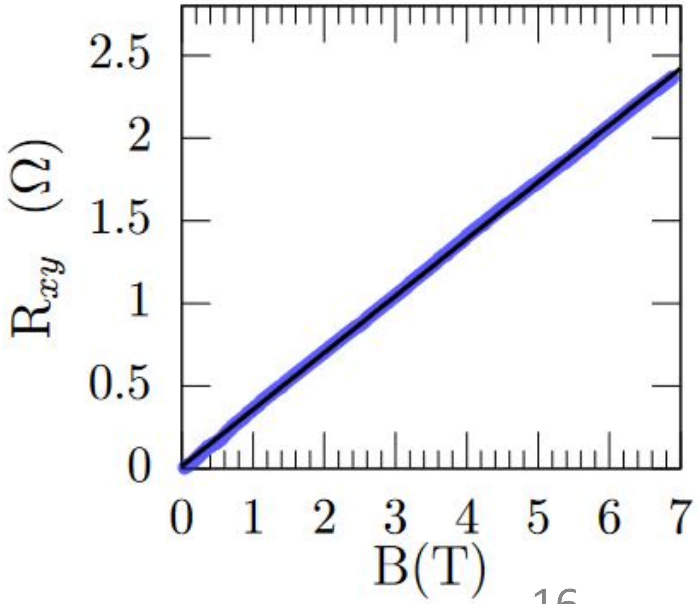

Magnetoconductance

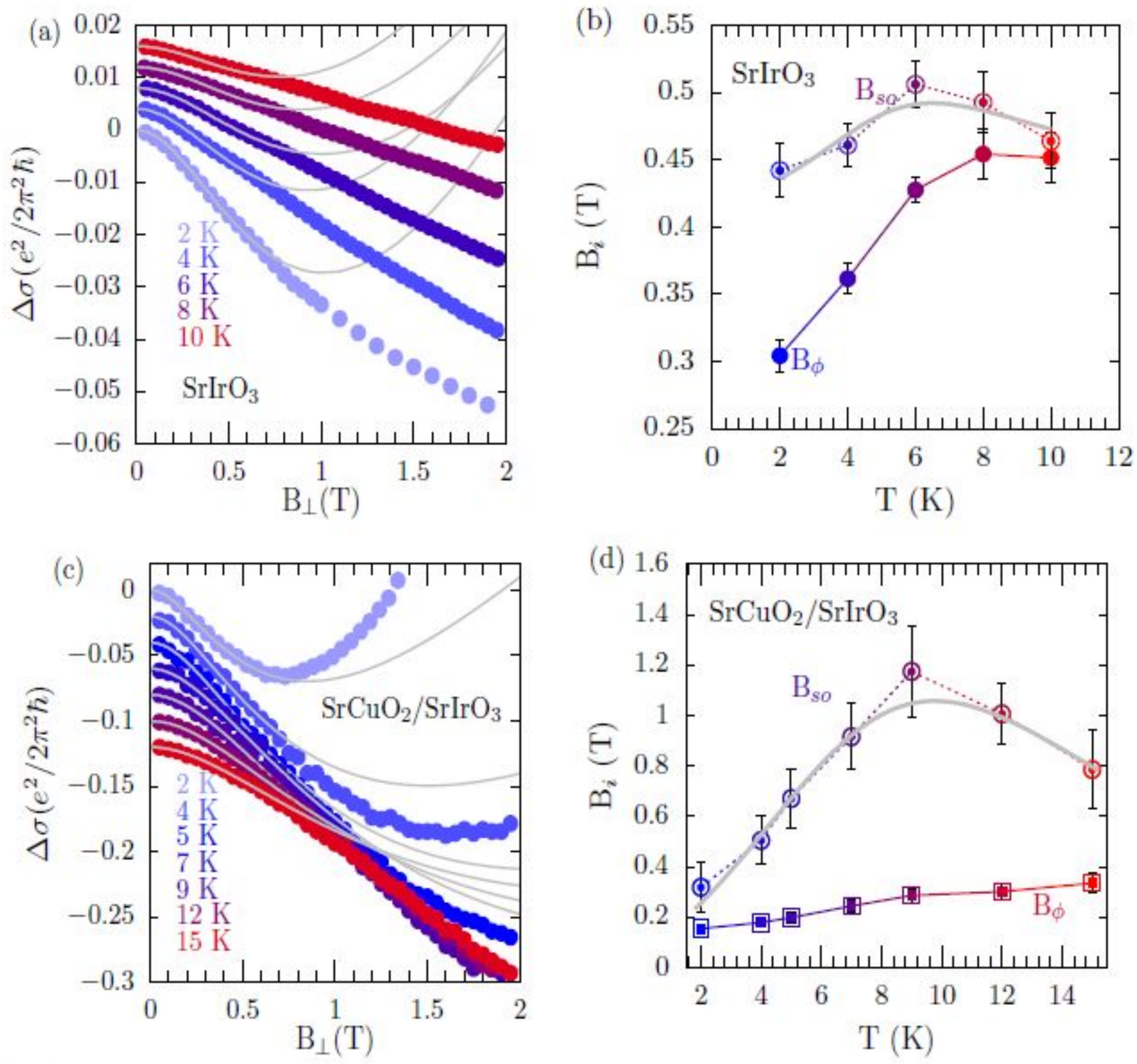

Hikami-Larkin-Nagoka equation

$$\Delta\sigma(B_\perp) = -\frac{e^2}{2\pi^2\hbar}\Bigg[\Big\{\psi(1/2 + B_e/B_\perp) + \ln(B_\perp/B_e)\Big\} + \frac{1}{2}\Big\{\psi(1/2 + B_\phi/B_\perp) + \ln(B_\perp/B_\phi)\Big\} - \frac{3}{2}\Big\{\psi\Big(1/2 + \frac{B_\phi + B_{so}}{B_\perp}\Big) + \ln\Big(\frac{B_\perp}{B_\phi + B_{so}}\Big)\Big\}\Bigg] \quad (1)$$

$$B_i = \hbar/4el_i^2,$$

$$B_\phi(\propto l_\phi^{-2})$$

$$l_\phi^{-2} = l_{\phi\ ideal}^{-2} + l_m^{-2}$$

l_ϕ~22nm(2K,l_ϕ~19nm(10K):SIO

l_ϕ~30nm(2K), l_ϕ~25nm(10K:SCO/SIO)

- Quenching of magnetic impurity scattering

S. Jana *et al.*, Phys. Rev. B 107, 134415 (2023)

Unusual B_{so} variation

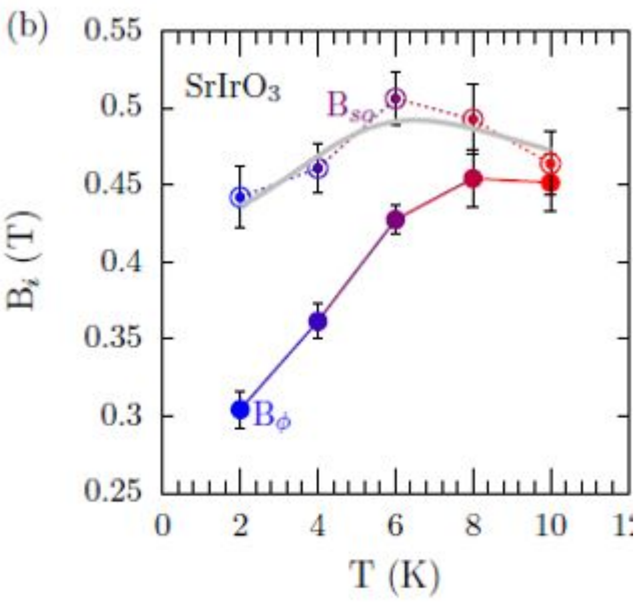

Eliott-Yafet type spin-orbit scattering

$$\frac{1}{\tau_{so}^{EY}} = \left(\frac{\lambda_{so}}{\Delta E}\right)^2 \frac{1}{\tau_e}$$

F. Simon *et al.*,PRL 101, 177003 (2008)

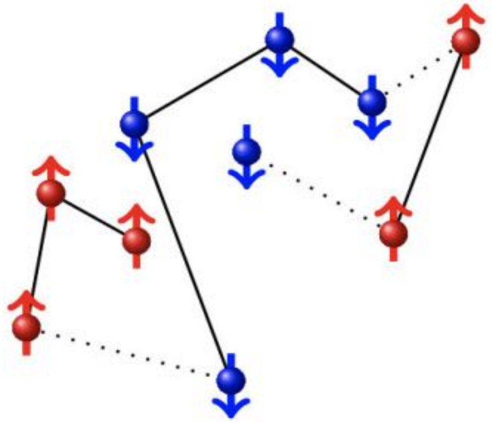

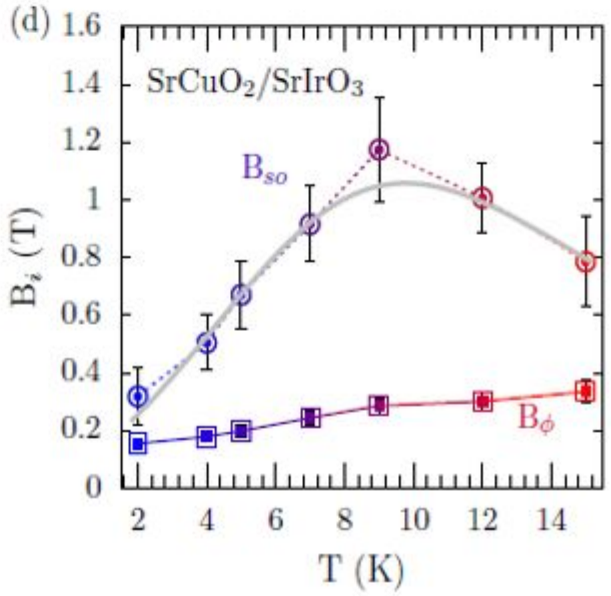

Flat electronic continuum extending at least up to 1000 cm^{-1} (~125 meV)

Strange semimetal dynamics in $SrIrO_3$

K. Sen *et al.,* Nat. Comm. 11,4270 (2020)

$$\tau_{FL}^{-1} \propto \frac{1}{\varepsilon_F}\left(\varepsilon^2 + k_B^2 T^2\right); \; \tau_{NFL}^{-1} \propto \left[\left(\varepsilon^2 + k_B^2 T^2\right)\right]^\alpha; \; \tau_{MFL}^{-1} \propto \left(\frac{\varepsilon + k_B T}{\log(\omega_c/T)}\right)$$

Antiferromagnetic proxmity enhances marginal FL behaviour

Longitudinal magnetoconductance (*B* ‖I)

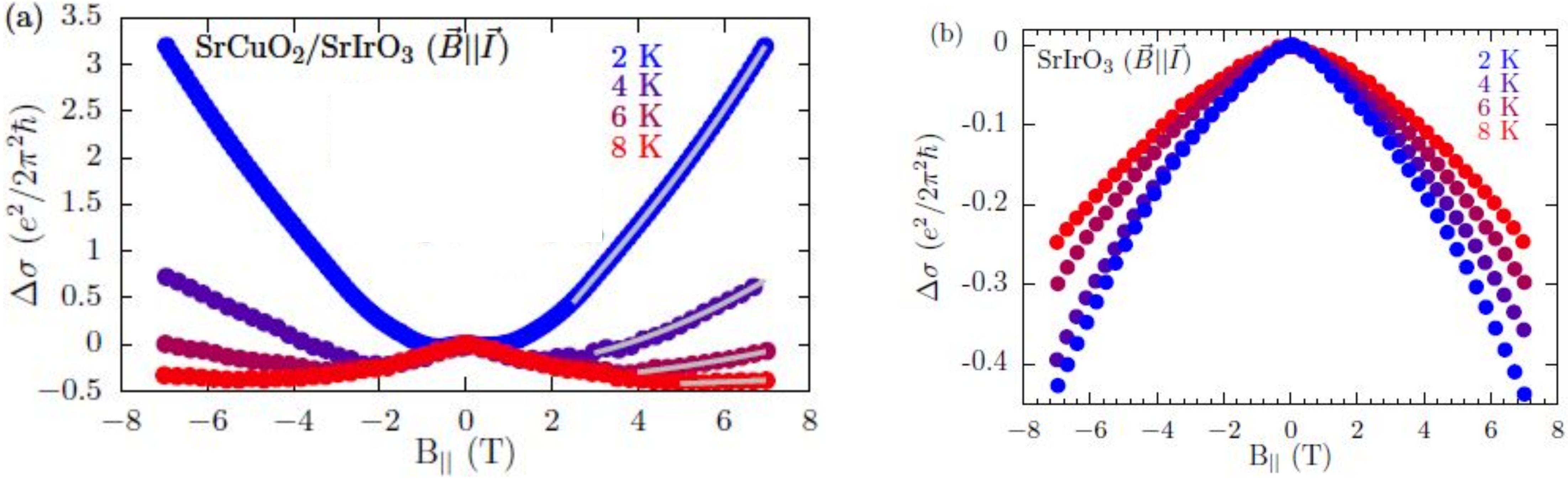

Chiral anomaly induced positive magnetoresistance

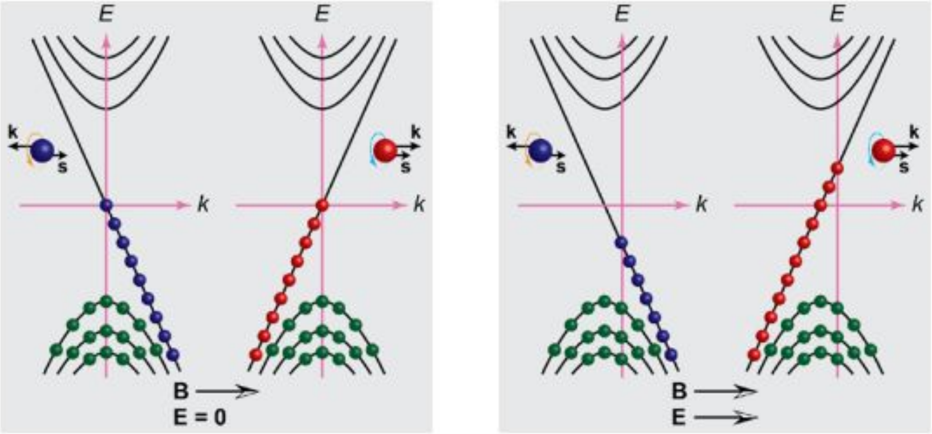

Li *et al.*,Nuclear Physics A 956,107 (2016)

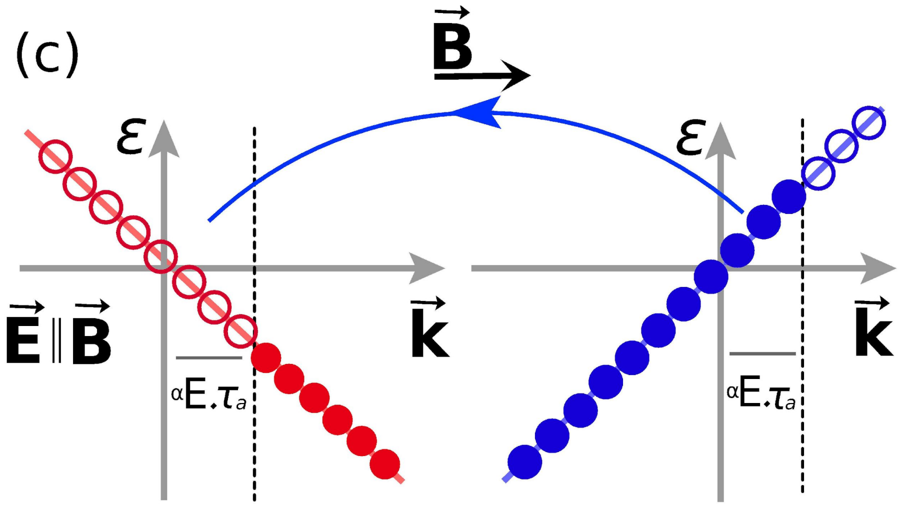

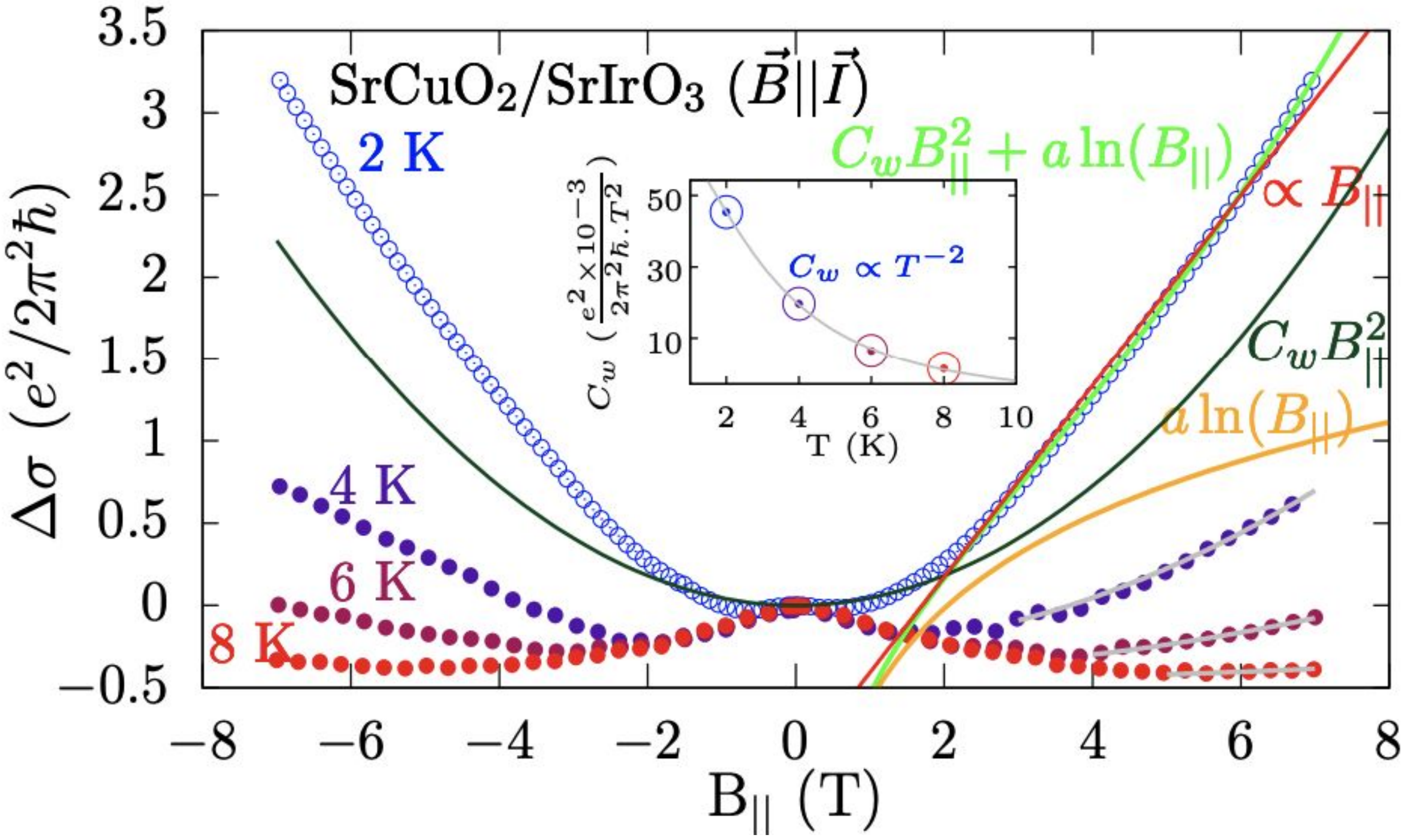

$$\Delta\sigma_{chiral}(B_{||},T) = \frac{3e^4 v_F^3}{8\pi^4\hbar^2 c}\cdot\frac{\tau_a}{T^2+(\mu/\pi)^2}\cdot B_{||}^2 = C_w B_{||}^2$$

S. Jana et al.,Phys. Rev. B 107, 134415 (2023)

Summary -I

- **Antiferromagnetic proximity effect paves an avenue to preserve the nontrivial quantum phenomena in complex materials by circumventing the detrimental effect of unintended magnetic impurity scattering.**

- **It will be useful as an effective way to control undesired spin relaxation by magnetic impurity scattering in the field of spintronics.**

Role of spin dimensionality on magnetic ordering in 2D systems

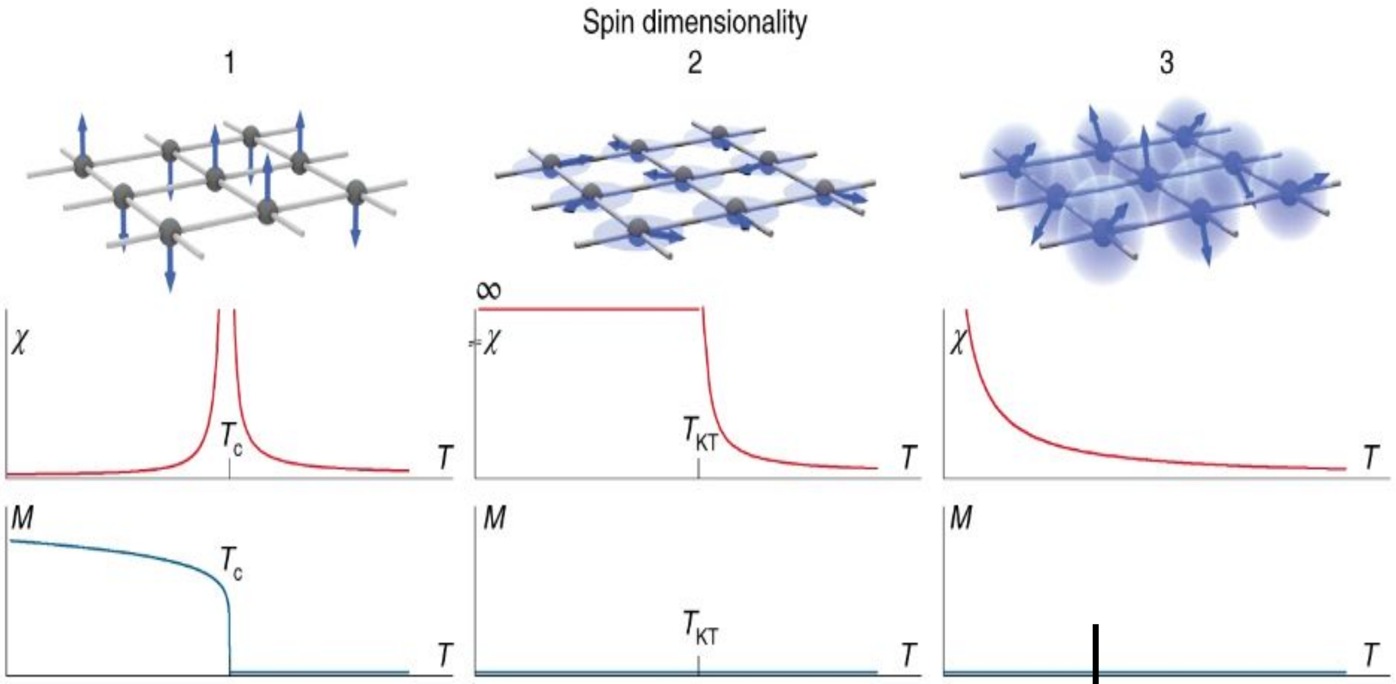

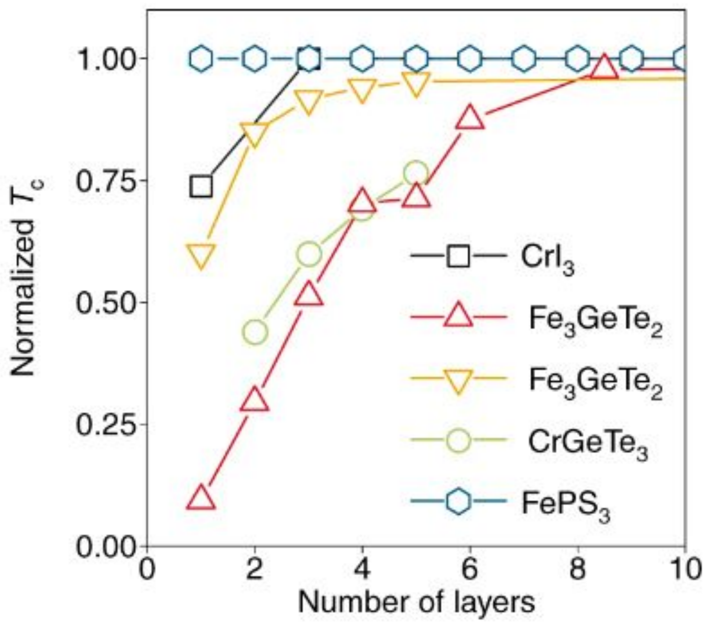

Nature Nanotechnology 14, 408 (2019)

Mermin-Wagner theorem forbids spontaneous symmetry breaking at finite temperature for 2D isotropic Heisenberg system with short range interaction **(PRL 17,1133 (1966))**

Note: Anisotropy, long range interaction (e.g. dipolar)

Quasi 2D Heisenberg Magnet

- Quasi-2D magnets are those magnetic materials where the magnetic interactions are strong within the plane, but extremely weak interlayer coupling (either by large separations or by competing exchange pathways).

- Quasi-2D magnets are not limited to vdW layered magnets (Ruddlesden-Popper perovskite magnets (K_2NiF_4 La_2CuO_4)

- For a Quasi 2D Heisenberg magnet, 2D magnetic correlation is expected to exist in each layer at higher temperature and upon cooling the correlation length grows exponentially with 1/T and an effective 3D long range magnetic ordering emerges at lower temperature.

- The 3D long range magnetic order in quasi 2D limit is closely linked with the strength of interlayer coupling and/or the underlying magnetic anisotropy.

Quasi 2D magnetic Organic-inorganic hybrid perovskites (OIHPs)

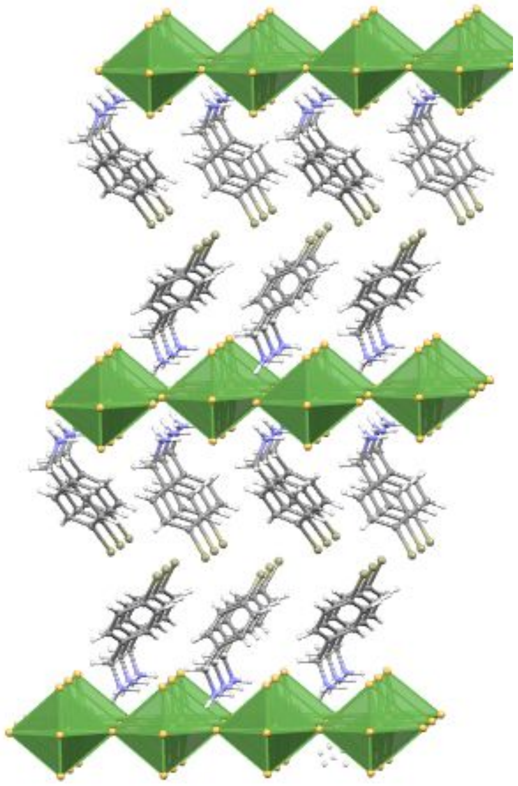

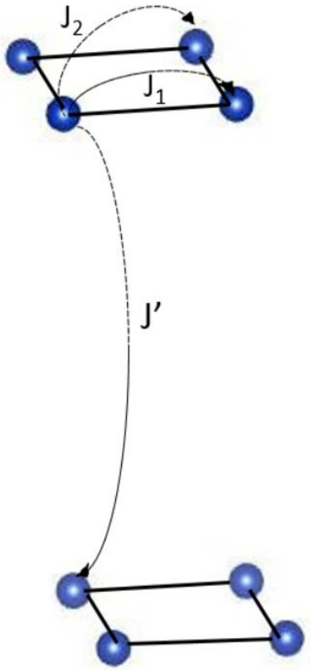

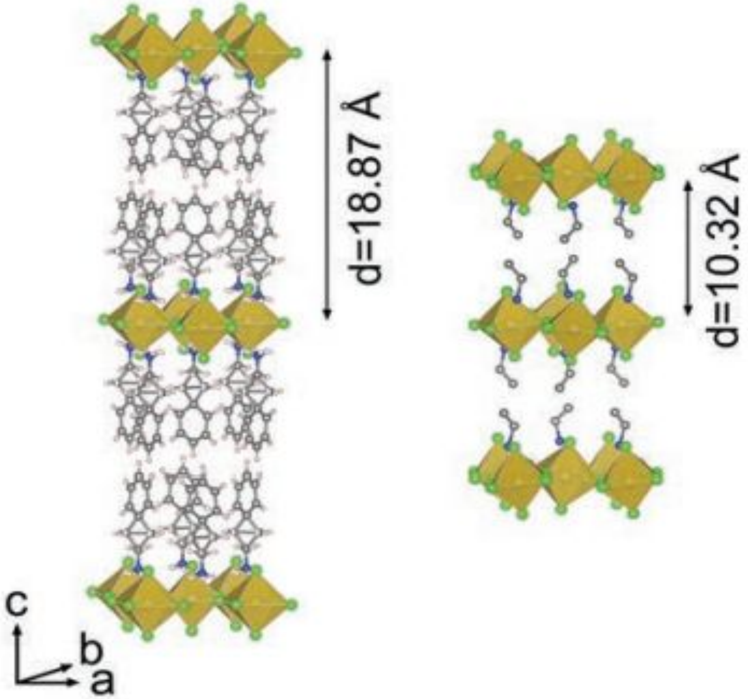

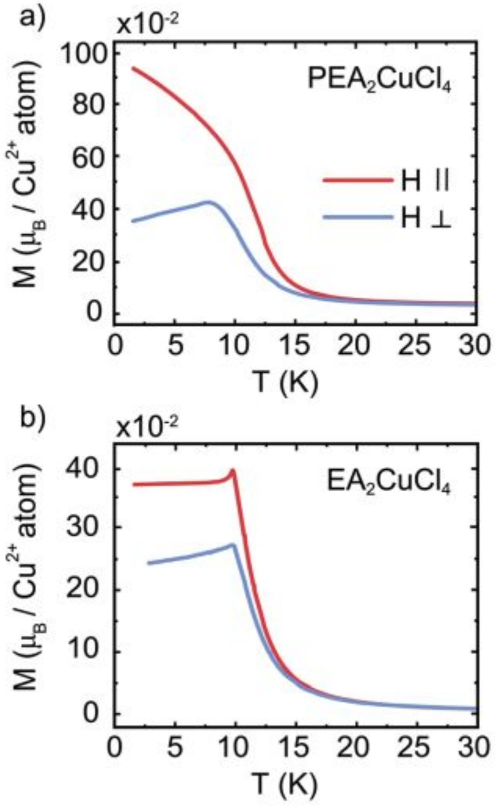

$J'/J \approx 10^{-2} - 10^{-6}$

Adv. Funct. Mater. 2207988 (2022)

M = Cu^{2+}, Cr^{2+}, Mn^{2+}, Fe^{2+}, Co^{2+}, and X = Cl, Br

Natural Superlattice

Cu based-Quasi 2D hybrid perovskites: Orbital ordering

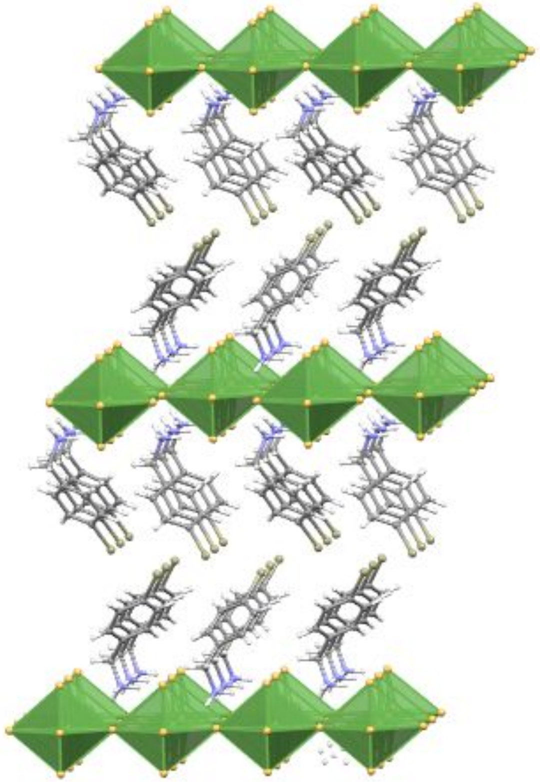

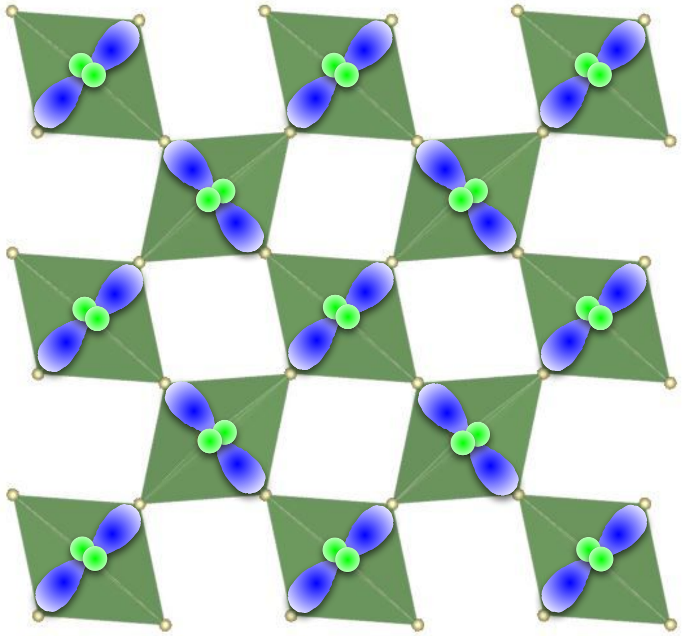

Anti-ferrodistortion in A_2CuX_4
Orbital ordering of $d_{x^2-z^2}$ and $d_{y^2-z^2}$

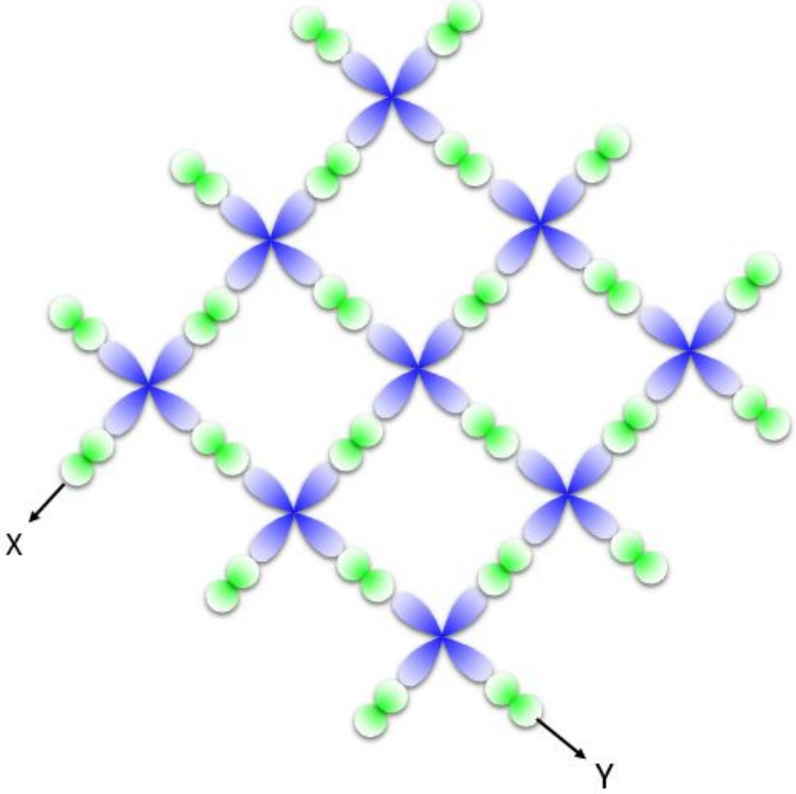

Orbital ordering $d_{x^2-y^2}$

PRB 94,184404 (2016)

Annu. Rev. Mater. Res. 48,111 (2018)

Chem. Mater. 24, 133 (2012)

Cross-type orbital ordering in $(C_6H_5CH_2CH_2NH_3)_2CuCl_4$

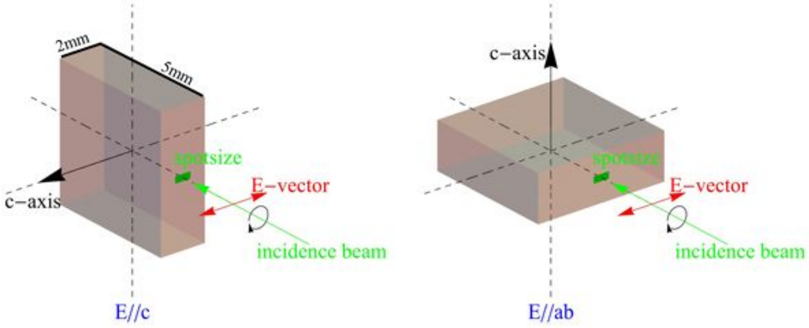

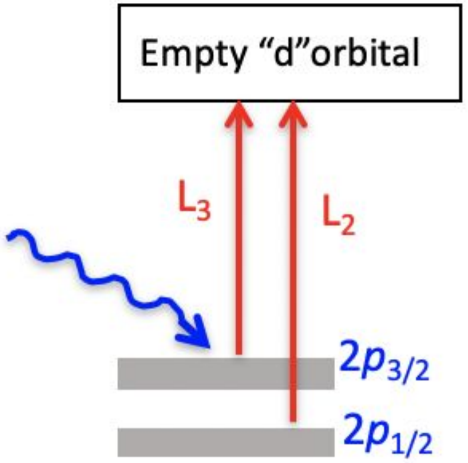

$$P_{if} \propto M^2 (1 - n(E_f)\, \delta[(\hbar\omega - (E_f - E_i)]$$

$$M^2 = \left|\langle f | P.A | i \rangle\right|^2 \rightarrow \left|\langle f | \varepsilon.r | i \rangle\right|^2$$

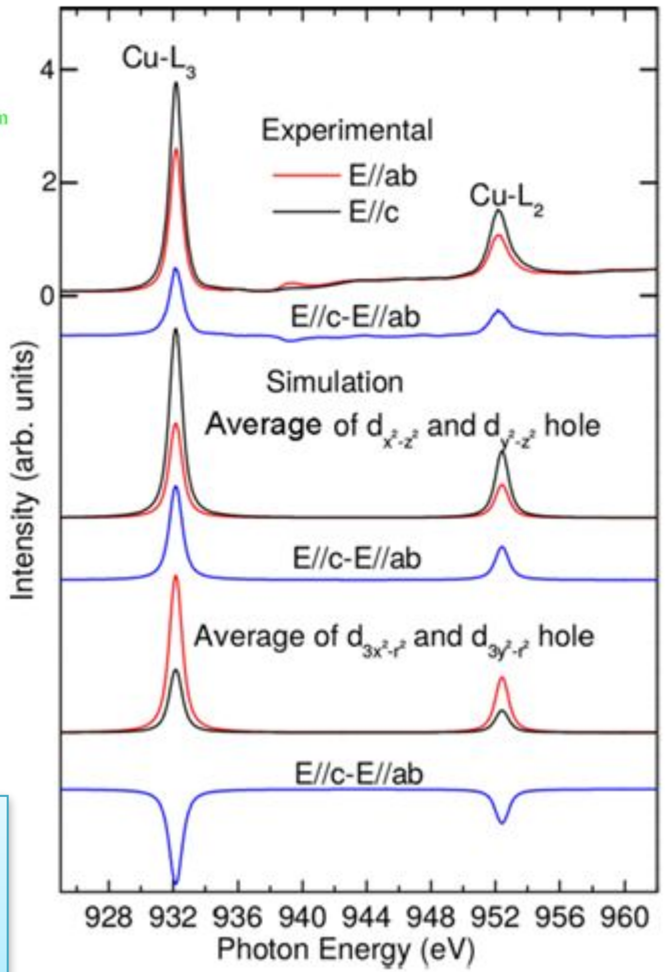

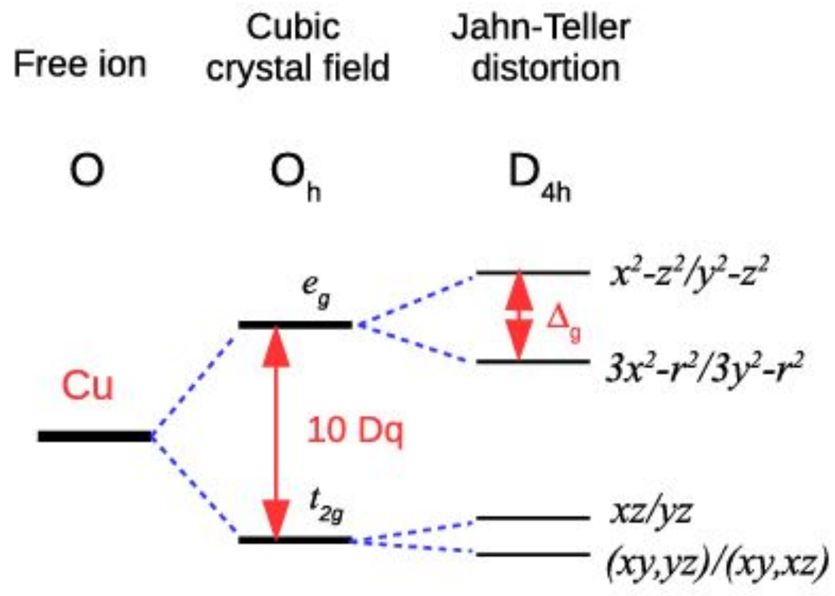

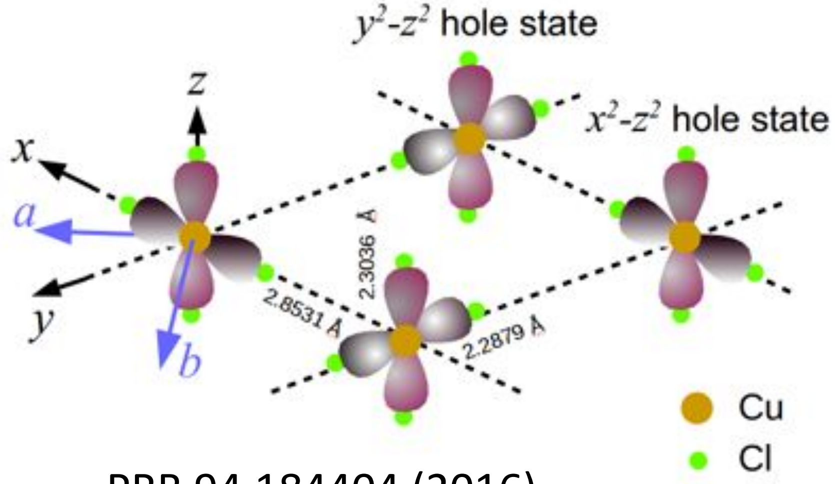

PRB 94,184404 (2016)

Crystal Structure of A_2CuX_4 (A= C_7H_9NBr, X = Cl, Br)

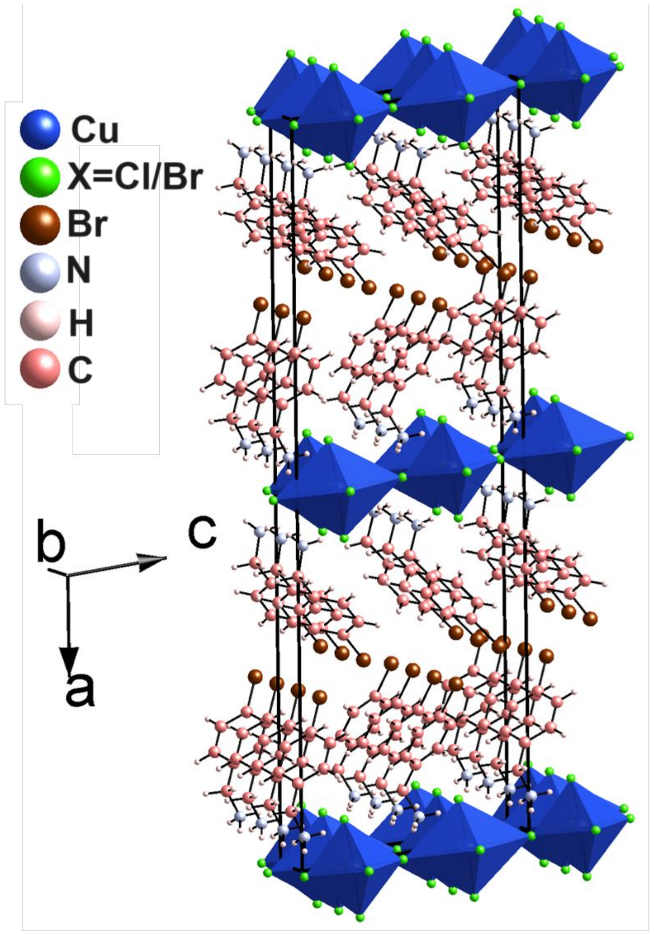

Monoclinic structure with polar space group Cc
(Inversion asymmetry)

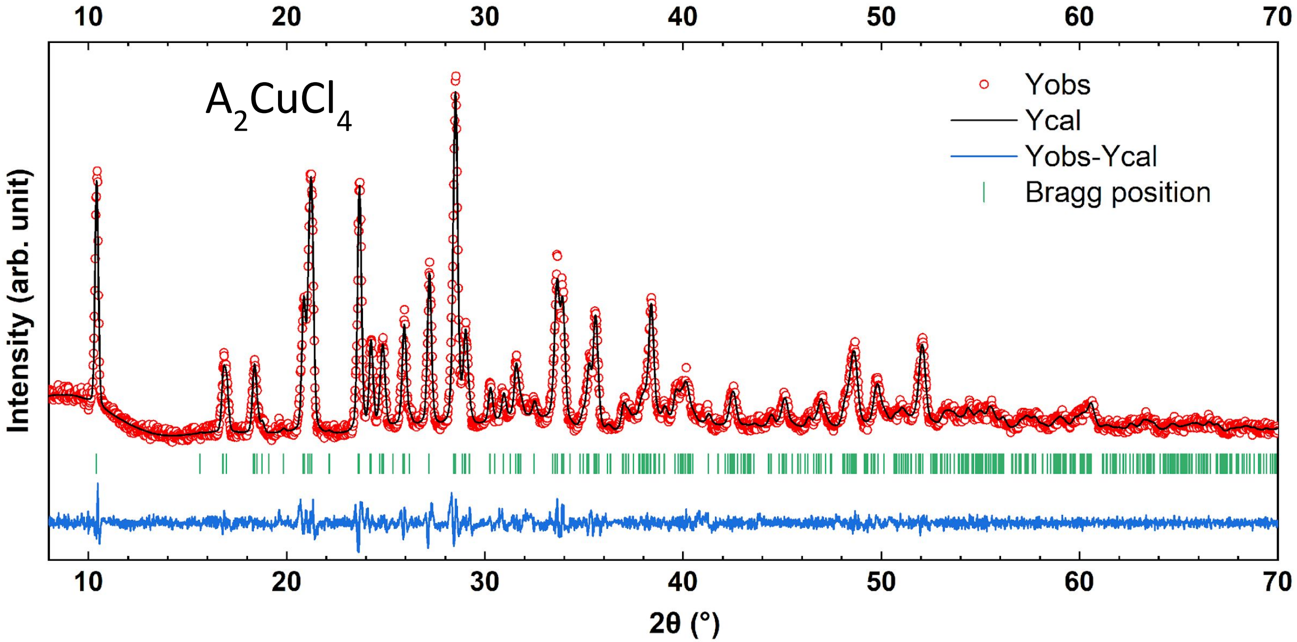

Lattice Parameter	a (Å)	b (Å)	c(Å)	β(°)
A_2CuCl_4	34.374(3)	5.288 (3)	10.666 (5)	98.676
A_2CuBr_4	33.794 (3)	5.522 (3)	11.044 (5)	99.262

Cu-Cu Distance	A_2CuCl_4	A_2CuBr_4
Intralayer	5.335 Å	5.524 Å
Interlayer	16.99 Å	16.67 Å

Contrasting Magnetism in A_2CuX_4 (X = Cl, Br)

IP : H ∥ c,   OP : H ⊥ bc

A_2CuCl_4 :

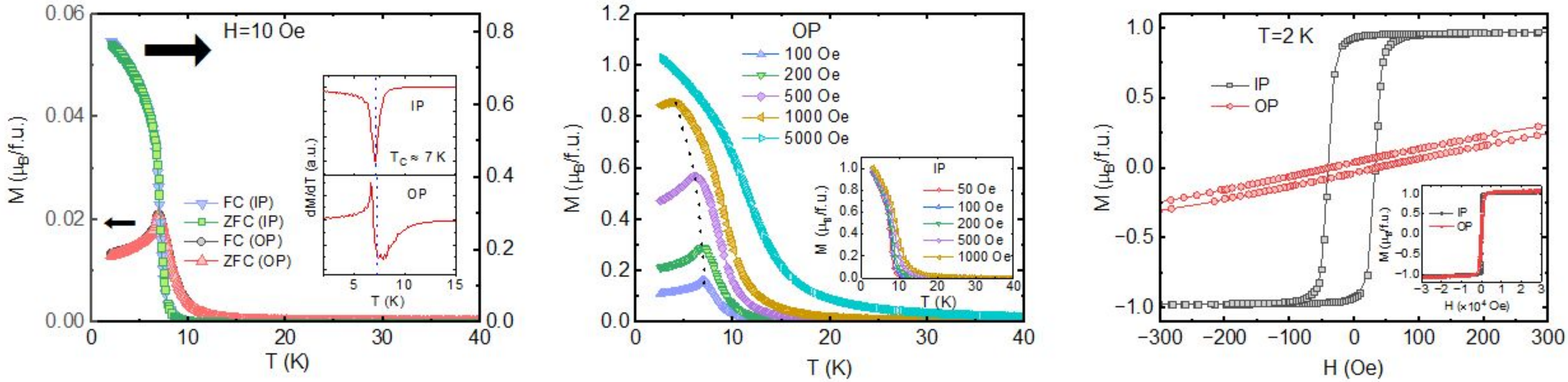

A_2CuBr_4 :

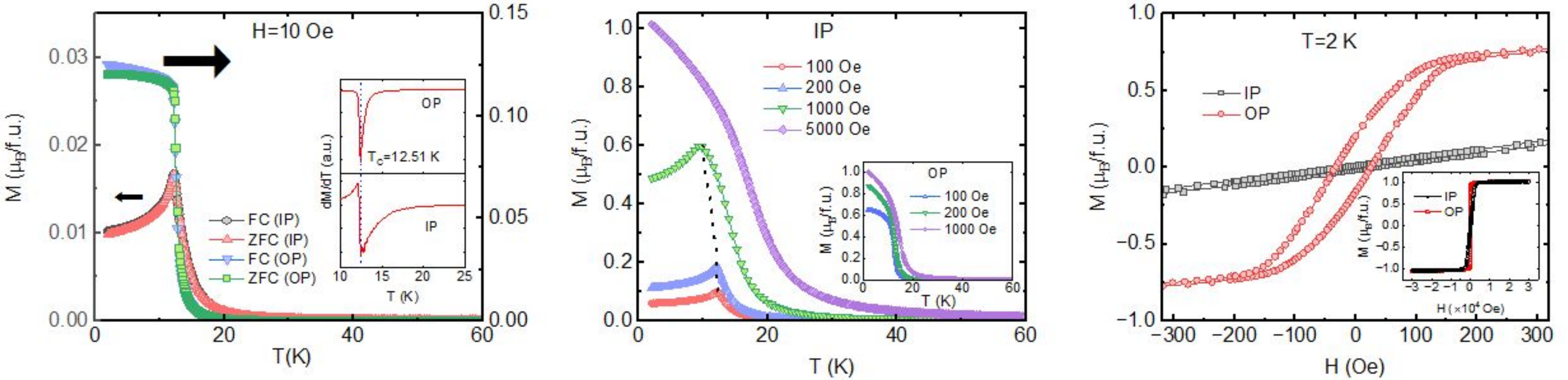

Underlying Dominant Ferromagnetic Interaction

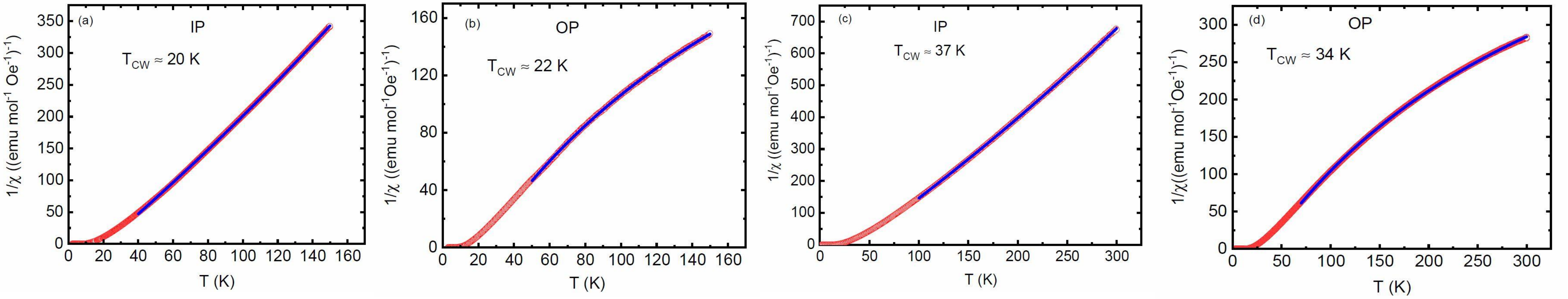

(A_2CuCl_4) (A_2CuBr_4)

Curie-Weiss law : $\chi = \chi_o + \frac{C}{T - T_{CW}}$

Orientations	χ_0 (emu mol^{-1}Oe^{-1})	C (emu mol^{-1}Oe^{-1} K)	T_{CW} (K)	T_C (K)
IP (A_2CuCl_4)	-3.6×10^{-4}	0.42	20	7
OP (A_2CuCl_4)	2×10^{-3}	0.54	22	7
IP (A_2CuBr_4)	-2.9×10^{-4}	0.45	37	12.5
OP (A_2CuBr_4)	1.5×10^{-3}	0.53	34	12.5

Strength of Intralayer Ferromagnetic Exchange

2D Heisenberg FM model: $$\chi = \frac{C}{T}\left[1 + \sum_{n=1}^{10} \frac{a_n}{2^n n!}\left(\frac{J}{k_B T}\right)^n\right]$$

A_2CuCl_4

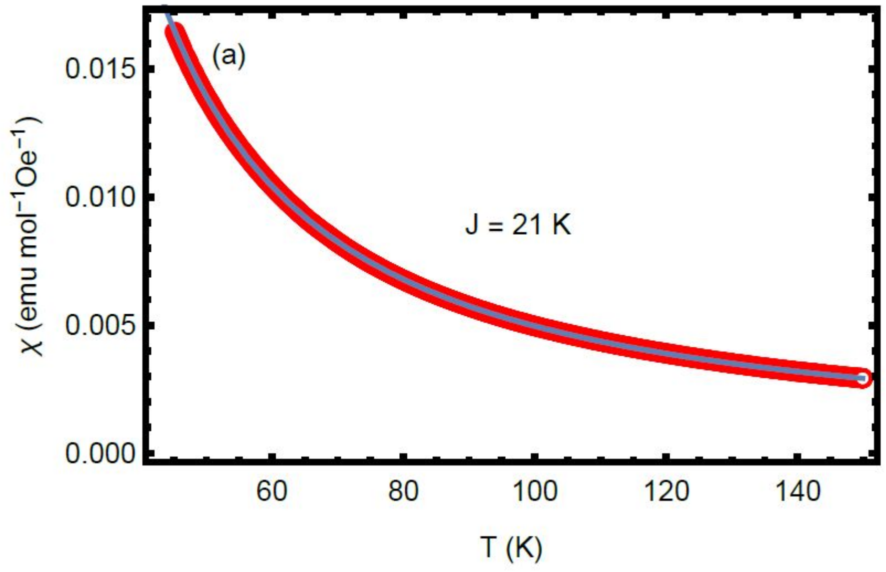

A_2CuBr_4

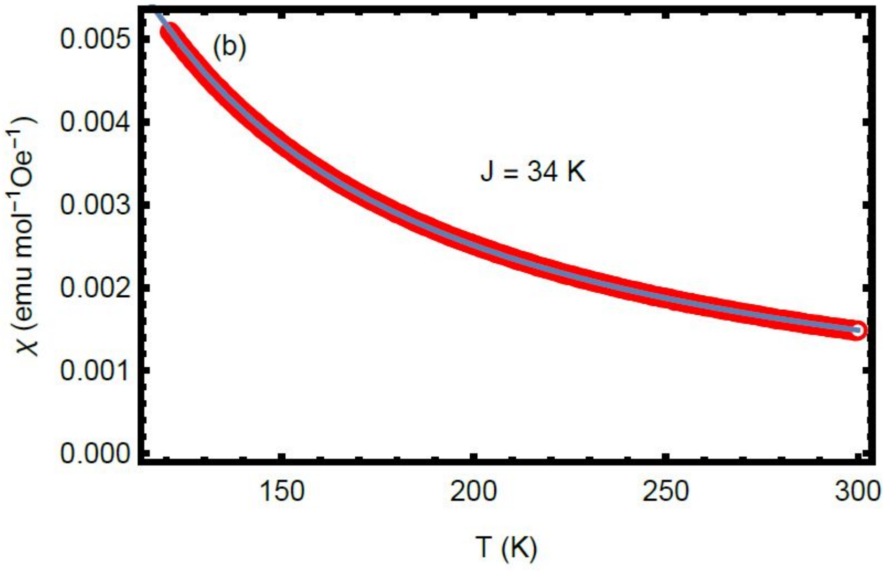

Interactions (meV)	J (experiment)	J (U = 4 eV)	J_2	MAE ($K_{\|\|}$)	K_{bc}
A_2CuCl_4	1.8	1.94	0.05	0.025	0.002
A_2CuBr_4	2.93	3.12	0.09	0.027	0.001

Contrasting Magnetism in A_2CuX_4 (X = Cl, Br)

IP : H ∥ c,   OP : H ⊥ bc

A_2CuCl_4 :

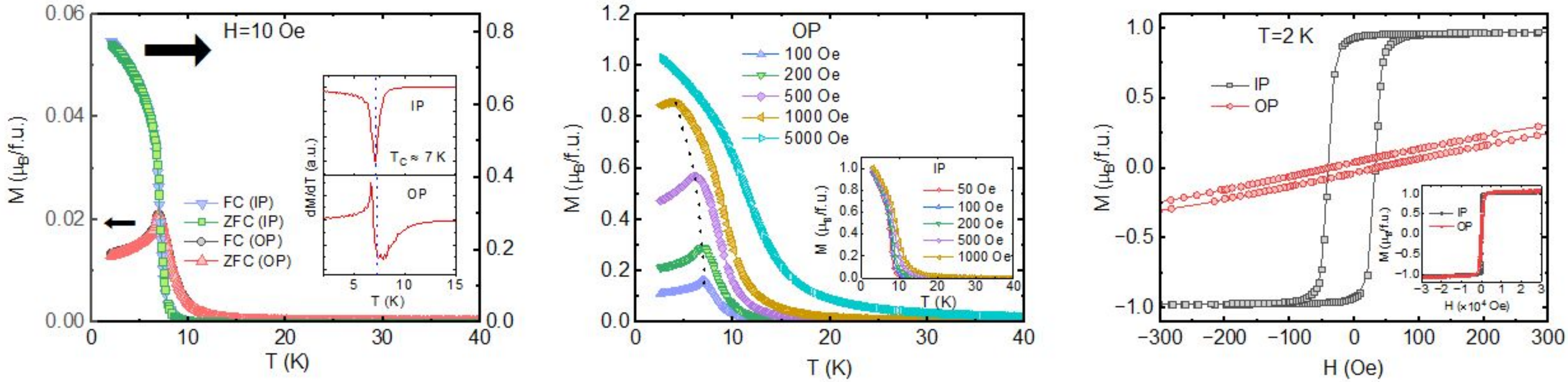

A_2CuBr_4 :

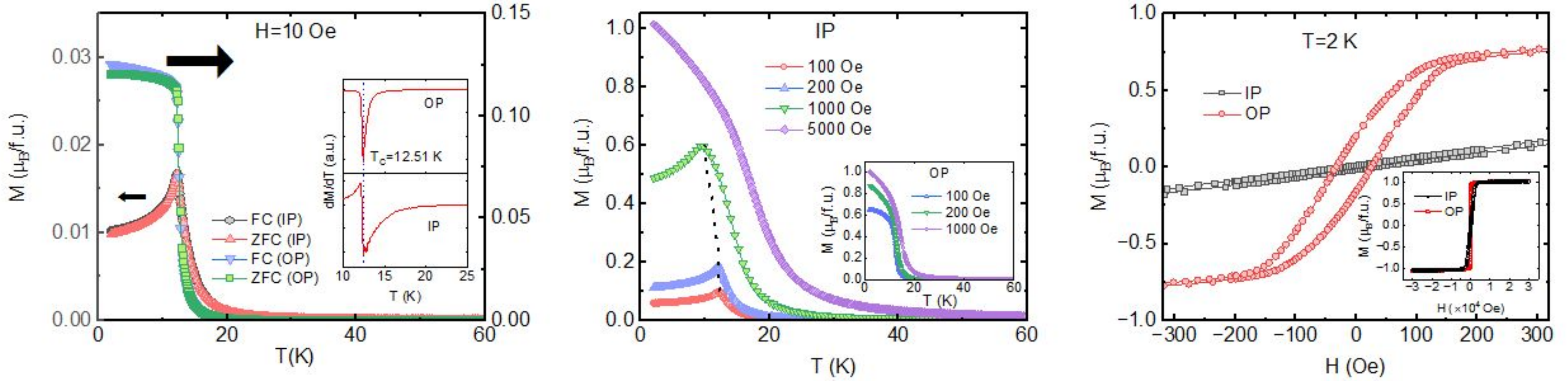

Examining the presence of Dzyaloshinskii-Moriya Interactions

$$|D_{ij}| \propto |E_{ACW\text{-}spiral} - E_{CW\text{-}spiral}| \qquad -\mathbf{D}_{ij} \cdot (\mathbf{S}_i \times \mathbf{S}_j)$$

Example helix along b-axis

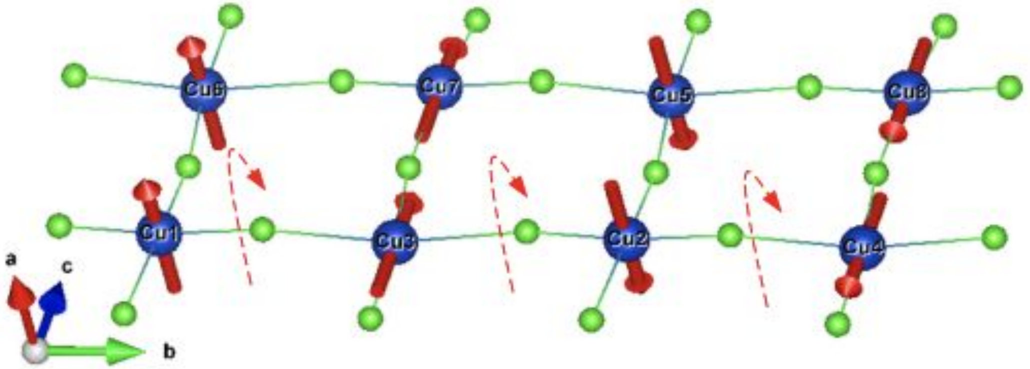

CW Helix

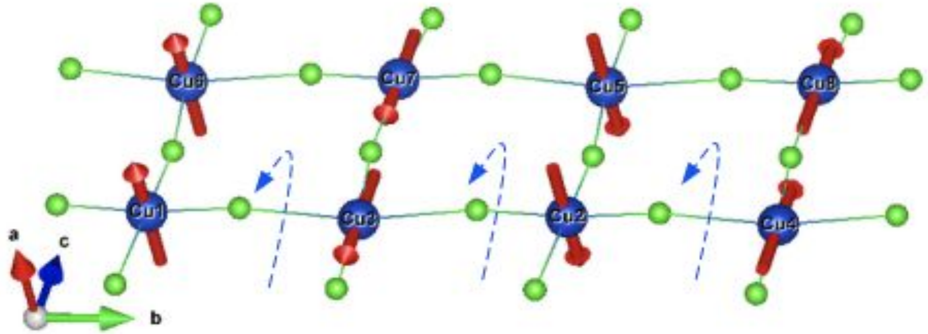

ACW Helix

Estimation of intraplane DMI

A_2CuCl_4 : spiral propagation direction along c- axis

$\mathbf{e}_{rot}$	Spiral clock-wise (CW)	Spiral anticlock-wise (ACW)	ΔE	$\mathbf{D}_{nn}$
X	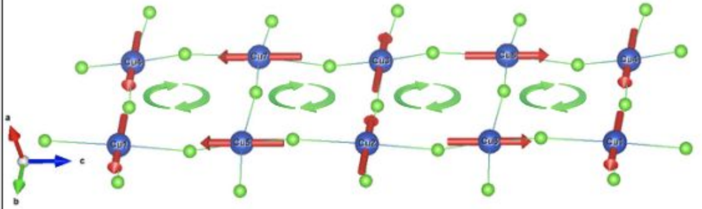	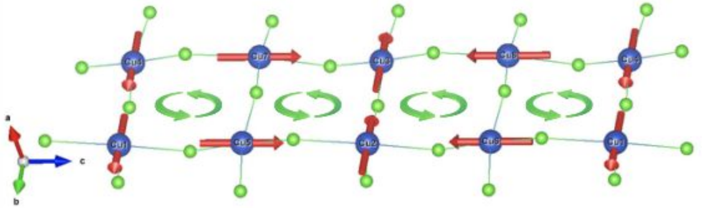	0.0019	0.0000
Y	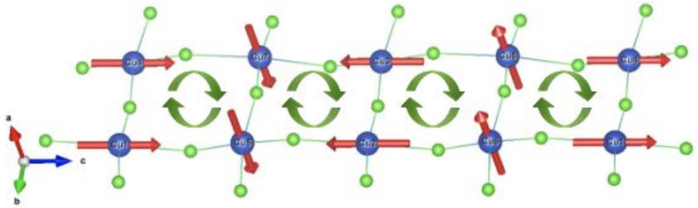	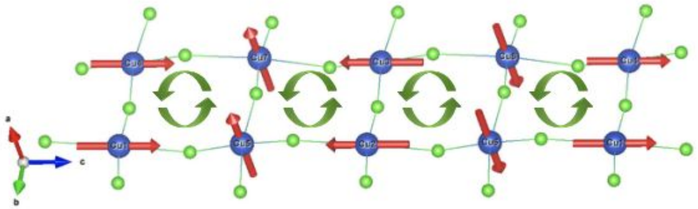	0.8256	0.0258
Z	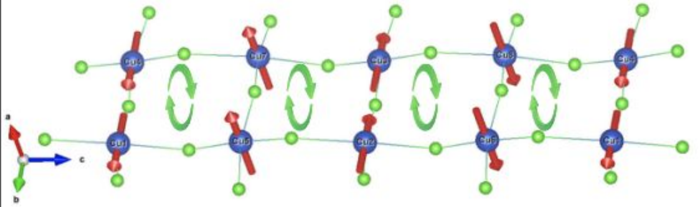	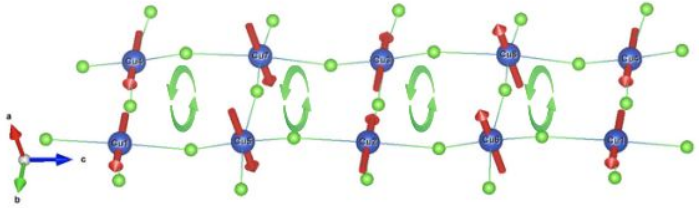	0.0067	0.0002

$\mathbf{e}_{rot}$ = rotation axis along cartesian axis ; $\Delta E = E_{CW} - E_{ACW}$ (*meV*) ; $\mathbf{D}_{nn}$ = nearest neighbour $|\mathbf{D}|$ (*meV*)

Strength of DMI and its Effect on local spin

A_2CuCl_4					
spin spiral along b			spin spiral along c		
$\mathbf{e}_{rot}$	ΔE (meV)	D (meV)	$\mathbf{e}_{rot}$	ΔE (meV)	D (meV)
(1,0,0)	0.035	0.001	(1,0,0)	0.002	0.000
(0,1,0)	0.007	0.000	(0,1,0)	0.826	0.026
(0,0,1)	0.062	0.002	(0,0,1)	0.007	0.000
$\vec{\mathbf{D}} = 0.001\hat{\mathbf{i}} + 0.000\hat{\mathbf{j}} + 0.002\hat{\mathbf{k}}$			$\vec{\mathbf{D}} = 0.000\hat{\mathbf{i}} + \underline{0.026\hat{\mathbf{j}}} + 0.000\hat{\mathbf{k}}$		
A_2CuBr_4					
spin spiral along b			spin spiral along c		
$\mathbf{e}_{rot}$	ΔE (meV)	D (meV)	$\mathbf{e}_{rot}$	ΔE (meV)	D (meV)
(1,0,0)	0.874	0.027	(1,0,0)	0.035	0.001
(0,1,0)	0.012	0.000	(0,1,0)	1.100	0.034
(0,0,1)	0.164	0.005	(0,0,1)	0.033	0.001
$\vec{\mathbf{D}} = \underline{0.027\hat{\mathbf{i}}} + 0.000\hat{\mathbf{j}} + 0.005\hat{\mathbf{k}}$			$\vec{\mathbf{D}} = 0.001\hat{\mathbf{i}} + \underline{0.034\hat{\mathbf{j}}} + 0.001\hat{\mathbf{k}}$		

A_2CuCl_4 : D_b = 0.026 meV

A_2CuCl_4 : D_b = 0.034 meV

D_{OP} = 0.027 meV

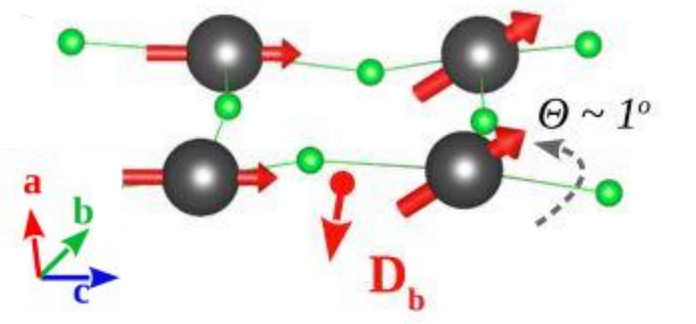

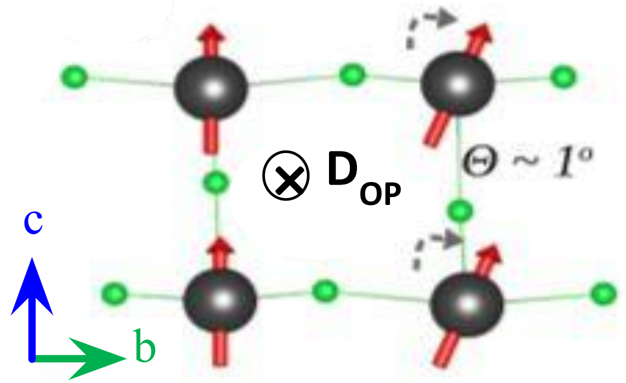

Proposed Spin structure

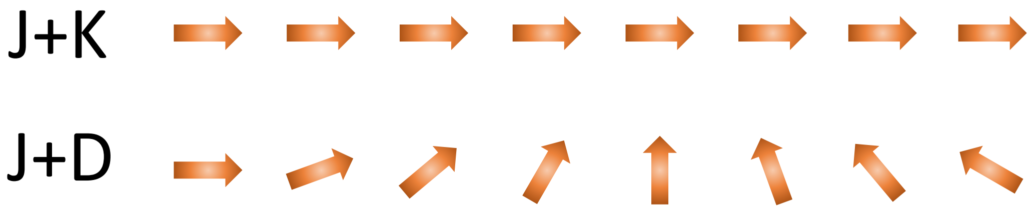

A_2CuCl_4 : Cu (easy axis along c-direction)

J_1 = 1.94 meV

MCA ($K_{\parallel}$) = 0.025 meV/Cu

D_b = 0.026 meV

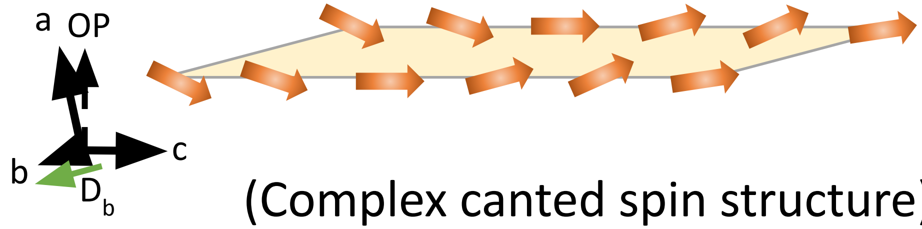

(Complex canted spin structure)

A_2CuBr_4 :

J= 3.12 meV

K_{bc} = 0.001 meV, D_{OP} = 0.027 meV

MCA ($K_{\parallel}$) = 0.027 meV, D_b = 0.034 meV

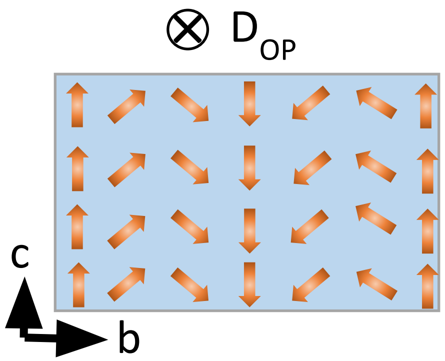

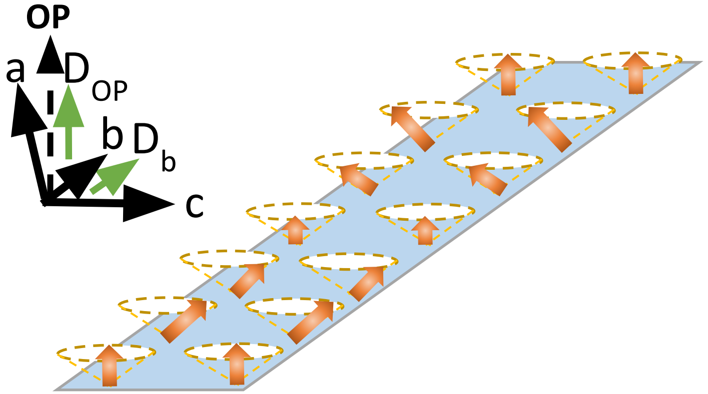

(Conical spiral spin structure)

A_2CuCl_4 : AC susceptibility measurements

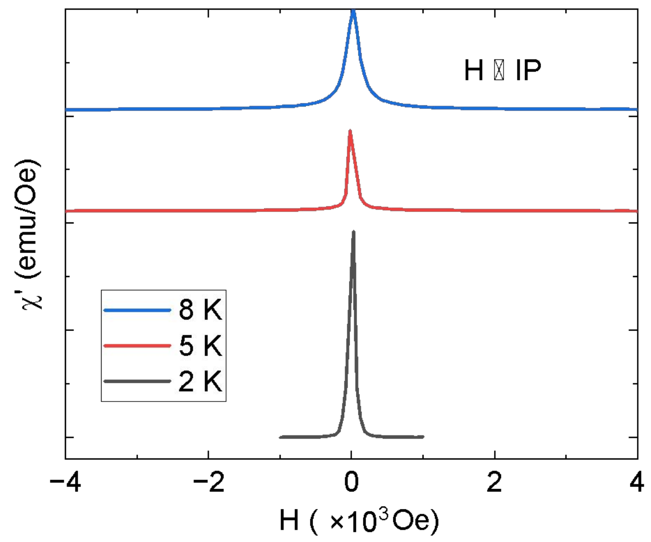

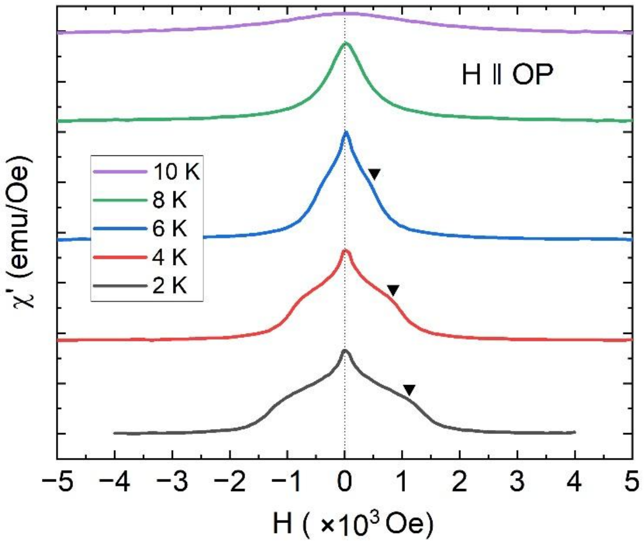

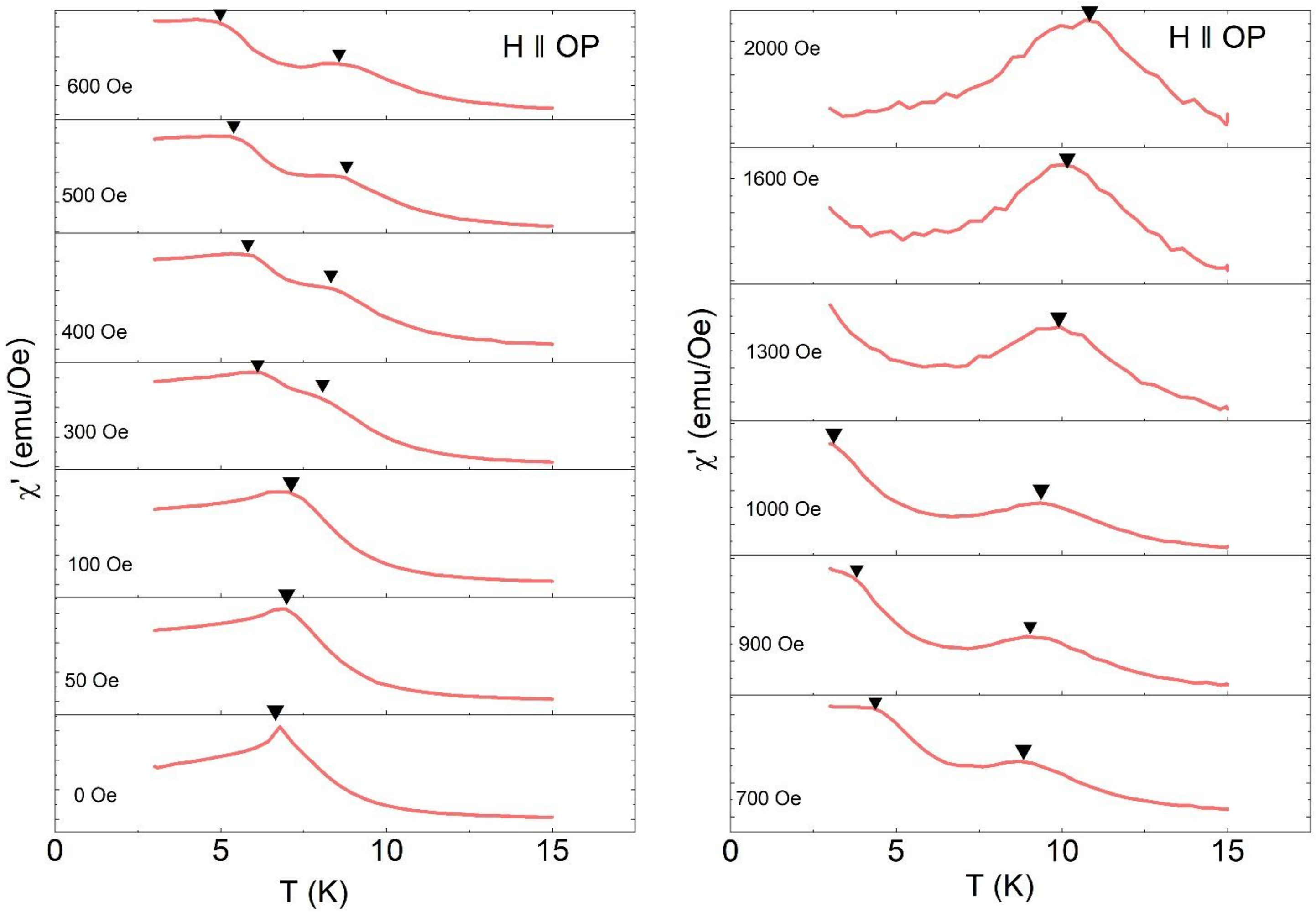

H_{ac} = 5 Oe, f = 599 Hz

A_2CuBr_4 : AC susceptibility measurements

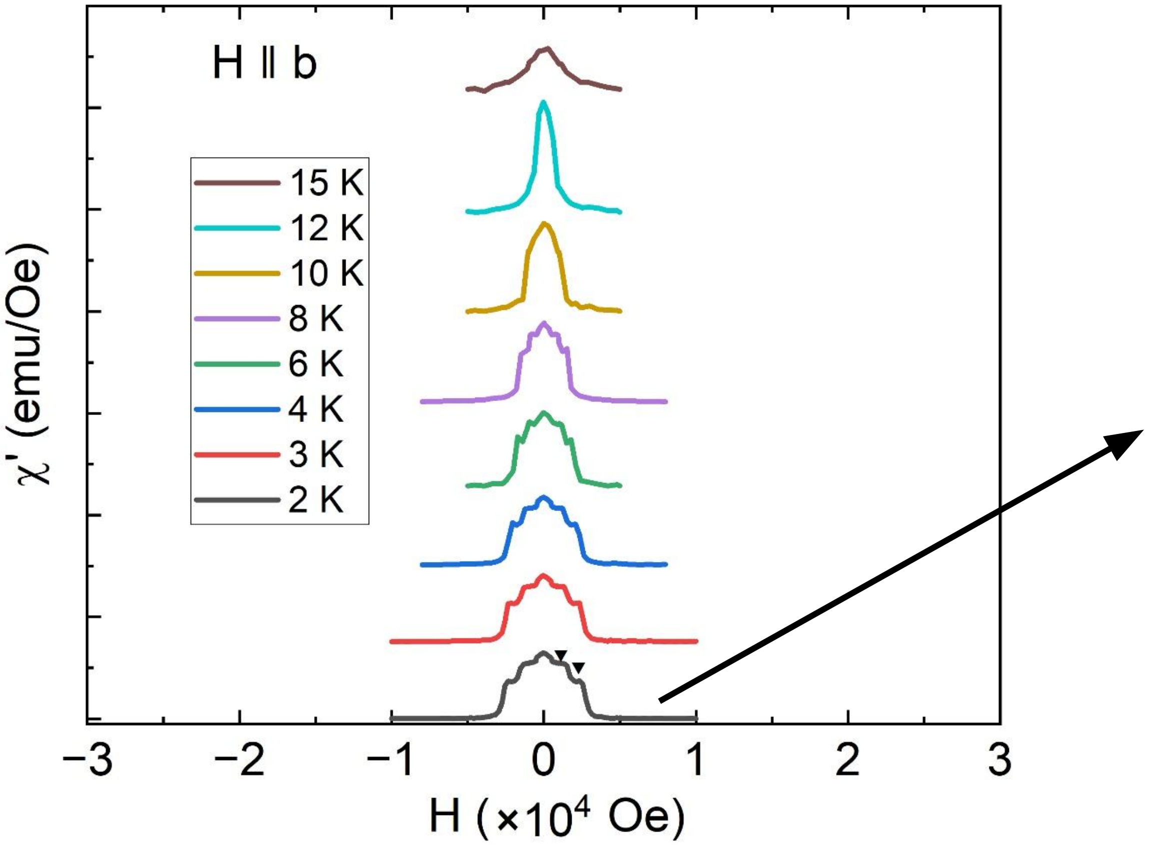

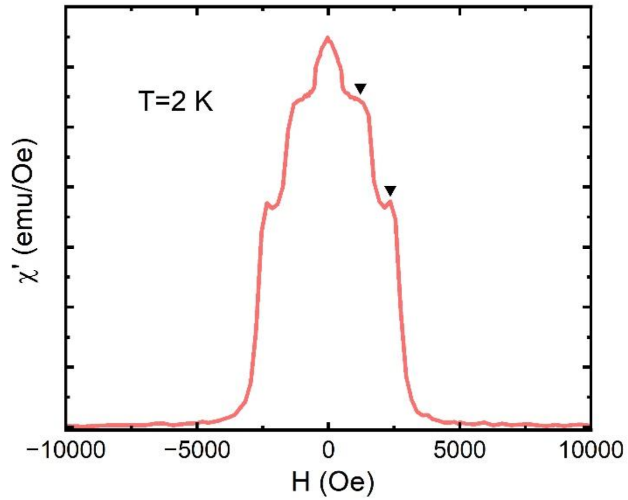

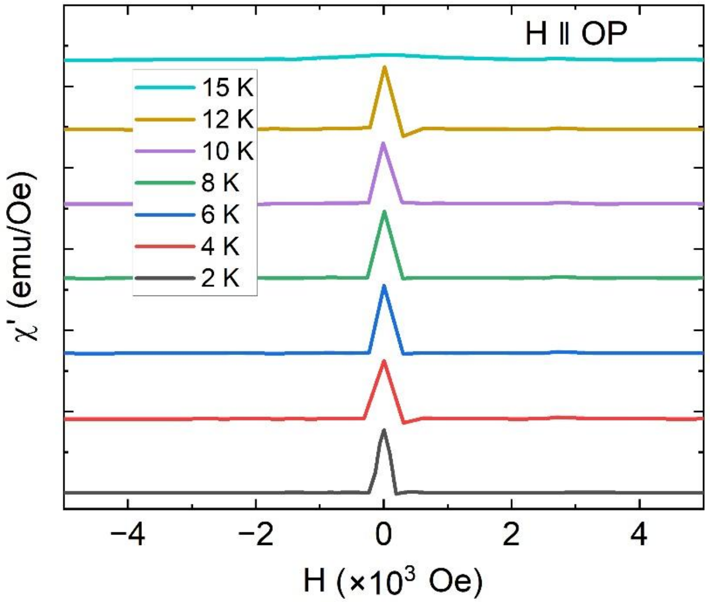

H_{ac} = 5 Oe, f = 599 Hz

A_2CuBr_4 : AC susceptibility measurements

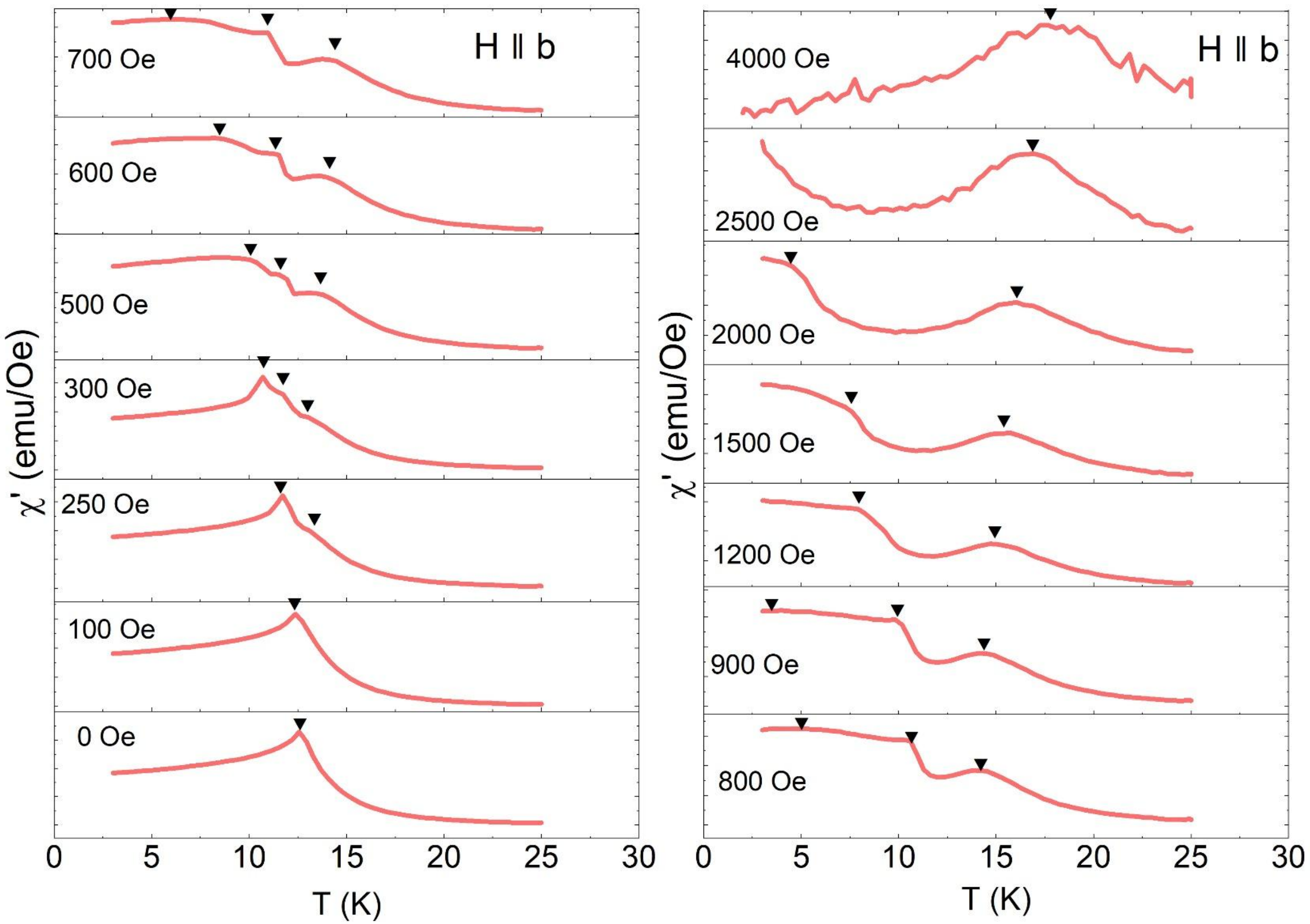

Our results so far….

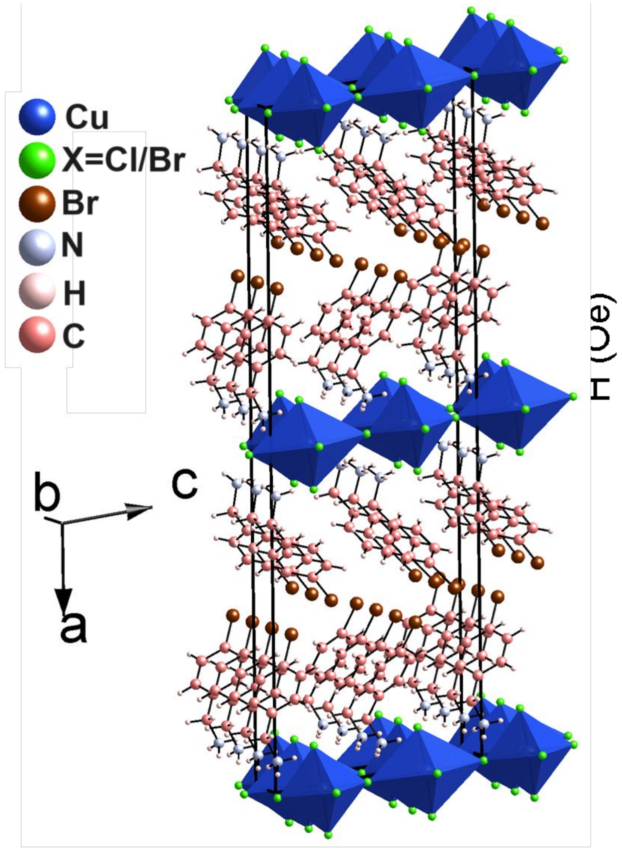

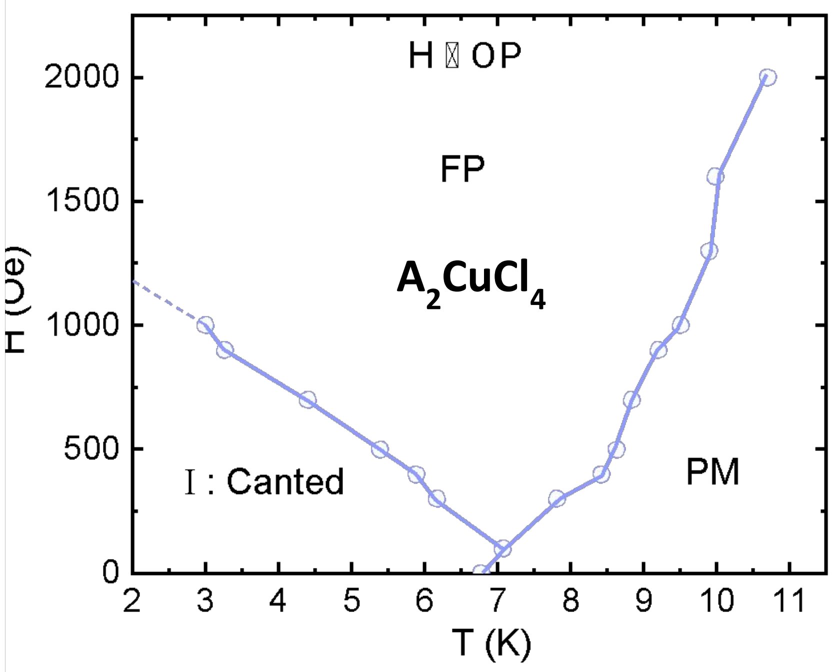

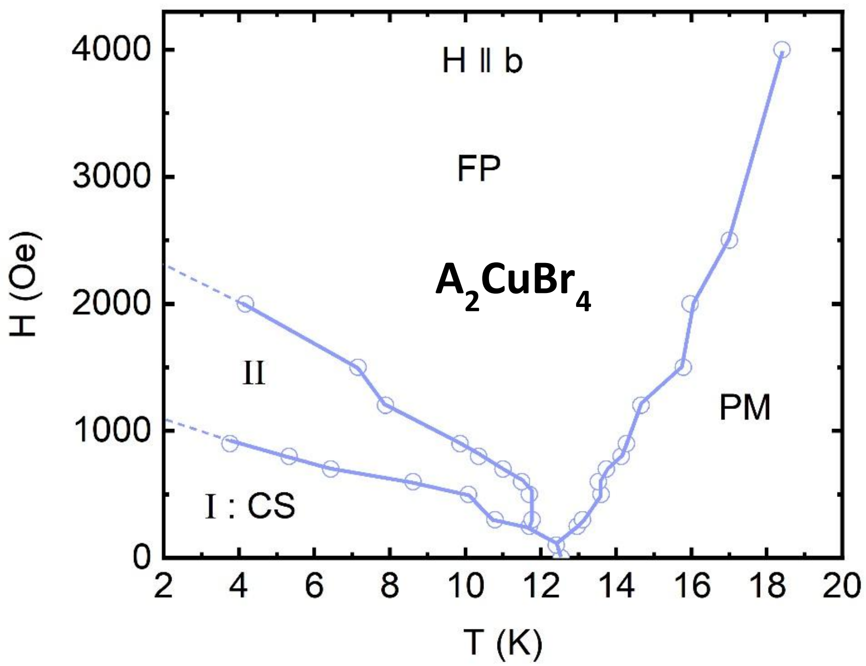

- We propose a canted and conical spiral (CS) magnetic ground state for Cl and Br analogues respectively.
- Our study essentially provides a paradigm to understand the occurrence of noncollinear magnetism and its ligand tunability in the realm of Cu based quasi 2D OIHPs.

Thank you for your attention!